

**PERFORMANCE ANALYSIS OF A PATCH
ANTENNA ARRAY FEED FOR A SATELLITE
C-BAND DISH ANTENNA**

Ibigbami, Oluwole Nelson

M.ENG./SEET/2007/1873

**DEPARTMENT OF ELECTRICAL AND COMPUTER ENGINEERING,
SCHOOL OF ENGINEERING AND ENGINEERING TECHNOLOGY,
FEDERAL UNIVERSITY OF TECHNOLOGY, MINNA,
NIGER STATE**

JANUARY, 2011

**PERFORMANCE ANALYSIS OF A PATCH
ANTENNA ARRAY FEED FOR A SATELLITE
C-BAND DISH ANTENNA**

Ibigbami, Oluwole Nelson

M.ENG./SEET/2007/1873

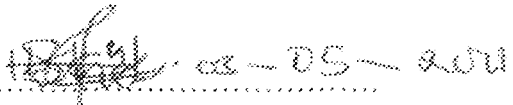
**A THESIS SUBMITTED TO THE POST GRADUATE SCHOOL,
FEDERAL UNIVERSITY OF TECHNOLOGY, MINNA,
IN PARTIAL FULFILMENT OF THE REQUIREMENTS FOR THE AWARD
OF MASTER OF ENGINEERING (M.ENG.) DEGREE
IN ELECTRICAL AND COMPUTER ENGINEERING
(COMMUNICATION ENGINEERING OPTION)**

DELENGBY
January, 2011

DECLARATION

I declare that this thesis "*Performance Analysis of a Patch Antenna Array Feed for a Satellite C-Band Dish Antenna*" was done by me and has never been presented elsewhere for the award of a Master Degree. It is the result of my own research work except for works cited in the references.

Ibigbami, Oluwole Nelson



Signature & Date

CERTIFICATION

This thesis titled: "*Performance Analysis of a Patch Antenna Array Feed for a Satellite C-Band Dish Antenna*", by Ibigbami Oluwole Nelson (M.Eng/SEET/2007/1873) meets the regulation governing the award of the degree of Master of Engineering (M.Eng) of the Federal University of Technology, Minna and is approved for its contribution to scientific and literary presentation.

ENGR. DR. Y. A. ADEDIRAN
SUPERVISOR


..... 5/12/2011
SIGNATURE & DATE

ENGR. A. G. RAJI
HEAD OF DEPARTMENT
ELECTRICAL AND COMPUTER ENGINEERING


..... (May 3, 2011)
SIGNATURE & DATE

ENGR. PROF. M.S. ABOLARIN
DEAN, SEET


..... 6/5/11
SIGNATURE & DATE

PROF. (Mrs.) S.N. ZUBAIRU
DEAN, POSTGRADUATE SCHOOL


..... 1/11/2011
SIGNATURE & DATE

DEDICATION

This thesis is dedicated to the memory of my late wife Musili Nike Ibigbami. May you continue to rest peacefully in the bosom of the Lord.

ACKNOWLEDGEMENTS

I wish to express my sincere gratitude to my supervisor, Dr. Y.A. Adediran for his fatherly role in the supervision of this work and for his excellent guidance which he always offered with enthusiasm and good spirits. His deep insights and professional knowledge were invaluable in making me aware of the numerous interesting new ideas related to my topic

I would also like to thank the following people for their various contributions to the success of this work, the head of department of Electrical and Computer Engineering, Engr. A.G. Raji; the department's team of internal examiners, Engr. J. Kolo and Engr. C. Alenoghena; the team of project presentation assessors, for the advice and guidance given to me during the project presentation; and the entire staff of the Electrical and Computer Engineering department.

I would also like to acknowledge the Dean School of Postgraduates, Prof. (Mrs.) S.N. Zubairu and The Dean School of Engineering, Prof. M.S Abolarin for their support and the deputy Dean of School of Engineering, Dr. O. Chakwu, for patiently proof reading this thesis.

I wish to express my appreciation to the management and staff of the Federal University of Technology, Minna for the enabling environment given to me in the course of my study and to the management and staff of the National Space Research and Development Agency (NASRDA) for sponsoring and allowing me to engage on this research work.

Last, but not the least, I would like to thank my family for just being there, giving me the strength and the much needed moral support

ABSTRACT

This research work proposes a patch antenna array as an alternative feed for dish antennas on board satellites to solve the weight problem constituted by conventional feed horns. An 8x1 linear, C-Band, circular patch antenna array configuration with a broadside radiation pattern is designed as feed for a dish antenna with F/D ratio of 0.36 corresponding to aperture illumination of 140° . Two approaches to the design were employed. The first approach was to maintain a constant uniform inter-element distance while varying the excitation amplitudes of the individual array elements using Genetic Algorithm (GA) to achieve minimum sidelobe levels. The second approach was to maintain constant, uniform excitation amplitudes for the individual array elements while varying the uniform inter-element distances to achieve a strong radiation on the effective aperture of the dish. From the graphs and simulations, it is observed that the total radiated power from the array feed decreases with increasing uniform inter-element distances for a uniform array element amplitude excitation. Optimum illumination efficiency and gain for the feed was achieved at an inter-element spacing of about 0.63 cm ($\lambda/8$). At this spacing, the simulated efficiency without considering all the other efficiency components is 49.6%. This is very competitive when compared to that achieved with conventional feeds for the same F/D ratio which is between 50-75%. The total weight of the feed is 91.3g and total array length is approximately 18.5cm which satisfies the conditions of reduced weight and dimensions required for on-board satellite applications where mass and size limitations are extremely strict.

TABLE OF CONTENTS

	Page
Title Page	ii
Declaration	iii
Certification	iv
Dedication	v
Acknowledgments	vi
Abstract	vii
Table of Contents	viii
List of Tables	xii
List of Figures	xiii
Abbreviations and Symbols	xvi
Symbols	xviii

CHAPTER ONE

1.0 INTRODUCTION	1
1.1 Antennas	1
1.1.1 Radiation from Antennas	1
1.1.2 Classification of Antennas	3
1.2 Patch Antennas	7

1.2.1	Patch Antenna Radiation Mechanism	10
1.2.2	Feeding Techniques for Patch Antennas	10
1.3	Patch Antenna Arrays	14
1.3.1	Parallel – Fed Patch Antenna Arrays	15
1.3.2	Series – Fed Patch Antenna Arrays	17
1.4	Statement of the Problem	18
1.5	Aims and Objectives	19
1.6	Project Scope	19

CHAPTER TWO

2.0	LITERATURE REVIEW	20
2.1	Dish Antenna Feeding System and Aperture Efficiency	20
2.1.1.	Illumination Taper	21
2.1.2.	Spillover	21
2.1.3.	Surface Error	22
2.1.4.	Focus	22
2.1.5.	Blocking	22
2.1.6.	The Cassegrain-feed	23
2.1.7.	The F/D ratio	24
2.2	Patch Antenna Feed for a Parabolic Reflector	24
2.3	Aperture Coupled Patch Antenna Array	27
2.4	Design of an 8X1 Square Patch Antenna Array	29
2.5	Design, Simulation and Tests of a Low-cost Patch Antenna Array	32

2.6	Genetic Algorithm Optimization for Circular Patch Antenna	34
2.6.1	Selection and Reproduction	34
2.6.2	Crossover	35
2.6.3	Mutation	35
2.7	Design of Patch Antennas for Satellite Application	37
2.8	Cylindrical Patch Antenna Array	39
2.9	Circular Patch Antenna Array for C-Band	41
2.10	Circular Patch Array Antenna for Ku-band	43
2.11	Design of a Circularly Polarized Patch Array	44

CHAPTER THREE

3.0	MATERIALS AND METHODS	47
3.1	The Single Patch Antenna Array Element	47
3.2	The Dish Antenna	50
3.3	The Patch Antenna Array Feed Design	51
3.3.1	Assumptions for the patch antenna array design	52
3.3.2	Modeling the inter-element distance	53
3.4	Genetic Algorithm Optimization of the Patch Antenna Array	54
3.4.1	Amplitude Tapering Using Genetic Algorithm	55
3.4.2	Step 1: Define Parameters, Objective Function	55
3.4.3	Step 2: Create Initial Population	57
3.4.4	Step 3: Evaluate Objective Function	58
3.4.5	Step 4: Selection	59

3.4.6	Step 5: Crossover and Mutation	60
3.4.7	Step 6: Elitist Model	61
3.4.8	Step 7: Stop Criteria and Final Result	61
3.5	Varying Inter-Element Distance	63

CHAPTER FOUR

4.0	RESULTS	65
4.1	The patch antenna array feed (FNBW = Aperture Illumination = 140°)	65
4.2	The patch antenna array feed (FNBW = 180°)	67
4.3	The patch antenna array feed (Inter-element distance = 0.5cm)	70
4.4	The patch antenna array feed (Inter-element distance $> \lambda/4$)	71
4.5	Efficiency Computation	73

CHAPTER FIVE

5.0	DISCUSSION, CONCLUSION AND RECOMMENDATION	75
5.1	Introduction	75
5.2	Recommendations	76
5.2.1	Aperture illumination	76
5.2.2	Patch antenna element configuration	76
5.2.3	Array Configuration	77
REFERENCES		78
APPENDICES		80

LIST OF TABLES

Table		page
3.1	GA optimized normalized excitation amplitudes for the antenna array elements	63
5.1	Weight and Dimensions Comparison for the designed patch antenna array with conventional Radially Corrugated Horn feed for C-Band dish antenna	76

LIST OF FIGURES

Figure	page
1.1 Antenna as a region of transition between guided wave and free space wave	2
1.2 Examples of Aperture Antennas	5
1.3 Typical wire, aperture, and Patch antenna array configurations	7
1.4 Basic patch antenna configuration	8
1.5 Common Shapes of patch Antennas	9
1.6 Patch antenna in its basic form showing electric field distribution	10
1.7 Edge feed for patch antenna	11
1.8 Probe feed for patch antenna	12
1.9 Aperture coupled feed for patch antenna	13
1.10 Proximity coupled feed for patch antenna	13
1.11 Basic one-dimensional parallel fed patch antenna array: (a) Symmetrical configuration. (b) Asymmetrical configuration	16
1.12 Two-dimensional parallel fed patch antenna array	16
1.13 One-dimensional series-fed patch antenna arrays (a) Untransposed configuration (b) Transposed configuration	17
2.1 Typical Dish illumination for a dish antenna Illumination taper=10dB	22
2.2 Dish Antenna Cassegrain-feed arrangement	24
2.3 <i>S</i> -parameters of the patch antenna on air over an infinite ground plane	27

2.4	Top view of the 9-element antenna array	
2.5	Array configurations for $0.2\lambda_0$ patch widths	28
2.6	Simulated normalized power pattern for an equiphased nine element array	29
2.7	The Square Patch Element	30
2.8	The 8X1 Array Configuration	30
2.9	Gain Characteristics of an 8 element array	31
2.10	The 3x3 patch array that operates at 1.8 GHz, and with 35° beamwidth	33
2.11	Radiation patterns of the 3x3 patch at 1.8 GHz, left $\phi = 0^\circ$, right $\phi = 90^\circ$	33
2.12	Genetic Algorithm Process	35
2.13	Desired Frequency vs generations	37
2.14	3-D Plot of Directivity for receive antenna (right) and transmit antenna (left)	38
2.15	3D View of a 3-element array taken from the simulation software	40
2.16	Three-dimensional pattern of the patch antenna array $\phi = 0^\circ$ and $\phi = 90^\circ$ simulated with the HPHFSS 5.4	42
2.17	Geometry of the array of circular patch elements	43
2.18	The Simulated Gain of the circular patch array antenna	44
3.1	The single circular patch antenna element, $a = 0.88$ cm	48
3.2	Basic dish antenna geometry	50
3.3	The 8x1 patch antenna array feed for 6 GHz with inter-element spacing d (a) Top view, (b) Perspective view, (c) Wireframe view, (d) Bottom view	52
3.4	Aperture Illumination = First Null Beam Width (FNBW) = 140°	54

3.5	Flow chart of the Genetic Algorithm Process	55
3.6	Performance graph of the optimization process	62
3.7	Patch antenna array feed with inter-element distance 1.25cm Aperture Illumination = 140° , First Null Beam Width (FNBW) = 180°	64
4.1	Rectangular planar radiation pattern plot for 8X1 patch antenna array feed, $d = 0.67\text{cm}$	66
4.2	Polar radiation pattern plot for 8X1 patch antenna array feed, $d = 0.67\text{cm}$	66
4.3	3-D Radiation pattern plot for 8X1 patch antenna array feed, $d = 0.67\text{cm}$	67
4.4	Rectangular planar radiation pattern plot for 8X1 patch antenna array feed, $d = 0.625\text{cm}$	68
4.5	Polar radiation pattern plot for 8X1 patch antenna array feed, $d = 0.625\text{cm}$	68
4.6	3-D Radiation pattern plot for 8X1 patch antenna array feed, $d = 0.625\text{cm}$	69
4.7	Rectangular planar radiation pattern plot for 8X1 patch antenna array feed, $d = 0.5\text{cm}$	70
4.8	Polar radiation pattern plot for 8X1 patch antenna array feed, $d = 0.5\text{cm}$	70
4.9	3-D Radiation pattern plot for 8X1 patch antenna array feed, $d = 0.5\text{cm}$	71
4.10	Rectangular planar radiation pattern plot for 8X1 patch antenna array feed, $d = 1.35\text{cm}$	72
4.11	Polar radiation pattern plot for 8X1 patch antenna array feed, $d = 1.35\text{cm}$	72
4.12	3-D Radiation pattern plot for 8X1 patch antenna array feed, $d = 1.35\text{cm}$	73
4.13	Inter-element distance vs Radiated Power for the C-Band patch antenna array feed	74
4.14	Inter-element distance vs Aperture Efficiency for the C-Band patch antenna array feed	74

ABBREVIATIONS

<i>VHF</i>	very high frequency
<i>AM</i>	amplitude modulation
<i>HF</i>	High frequency
<i>UHF</i>	Ultra High Frequency
<i>MICs</i>	Microwave Integrated Circuits
<i>DRDC</i>	Defence Research and Development of Canada
<i>CanX-1</i>	Canadian picosatellite
<i>VSWR</i>	Voltage Standing Wave Ratio
<i>FDTD</i>	Finite-Difference Time-Domain
<i>GA</i>	Genetic Algorithm
<i>FEM</i>	Finite element method
<i>BWFN</i>	Beam width between first nulls
<i>FNBW</i>	First null beamwidth
<i>HPBW</i>	Half-power-beam width
<i>HPHFSS</i>	HP High Frequency Structure Simulator
<i>SLL</i>	Ratio of the maximum value of the largest side lobe to the maximum value of the main lobe

<i>ADS</i>	Advance Design System
<i>LEO</i>	Low Earth Orbit
<i>RHCP</i>	Right Hand Circular Polarization
<i>PCAAD</i>	Personal Computer Aided Antenna Design.

SYMBOLS

λ_0	Free space wavelength
L	length of rectangular patch
W	Width of rectangular patch
t	Thickness of patch
h	Thickness of substrate
ϵ_r	Dielectric constant
λ	wavelength
A_g	Geometrical area of the antenna aperture
η_t	Illumination efficiency of the aperture by the feed function ("taper")
η_s	Spillover efficiency of the feed (and sub reflector, if present)
η_r	Radiation efficiency of the reflector surface
η_p	Polarization efficiency of the feed-reflector combination
η_e	Surface error efficiency or scattering efficiency
η_f	Focus error efficiency (both lateral and axial defocus)
η_b	Blocking efficiency due to sub reflector or other obstruction
F	Focal Length of Parabolic Dish

D	Diameter of Parabolic Dish
θ_n	The first null beam width
v	Speed of electromagnetic radiation = 3×10^8 m/s
a_n	Amplitude excitation of the nth element.
β	Progressive phase shift between individual elements.
k	Wave number = $2\pi/\lambda$
d	Inter-element spacing
θ	Angle between the axis of the array (z-axis) and the radial vector from the origin to the observation point.
ψ	$kd \cos \theta + \beta$
θ_{3dB}	3 dB beamwidth

CHAPTER ONE

1.0 INTRODUCTION

1.1 Antenna

An antenna can be simply referred to as a transition device or a transducer that converts guided waves into free space waves or vice versa. An antenna converts bound circuit fields into propagating electromagnetic waves and, by reciprocity, collects power from passing electromagnetic waves (Milligan, 2005). An antenna converts alternating current oscillations to electromagnetic waves of the same frequency (Carr, 2001).

In addition to receiving or radiating energy, an antenna in an advanced wireless system is usually required to accentuate the radiation energy in some directions and suppress it in others. Thus, the antenna must also serve as a directional device in addition to a probing device (Balanis, 2005). It must then take various forms to meet the particular need at hand, and it may be a piece of conducting wire, an aperture, a patch, an array, a reflector, a lens, and so forth.

1.1.1 Radiation from Antennas

Time varying current in a conducting wire produces radiation because of acceleration or deceleration of charge. If there is no motion of charges in a wire, no radiation takes place since no flow of current occurs. Radiation will not occur even if charges are moving with uniform velocity along a straight wire. However, charges moving with uniform velocity along a curved or bent wire will produce radiation. If the charge is oscillating with time, then radiation occurs even along a straight wire (Kraus, 1988).

Figure 1.1 illustrates the concept of radiation from antennas. The source creates an electric field that is sinusoidal in nature. This, in turn, leads to the creation of electric lines of force which are tangential to the electric field. The free electrons on the conductors are forcibly displaced by the electric lines of force and the movement of these charges causes the flow of current which, in turn, leads to the creation of a magnetic field.

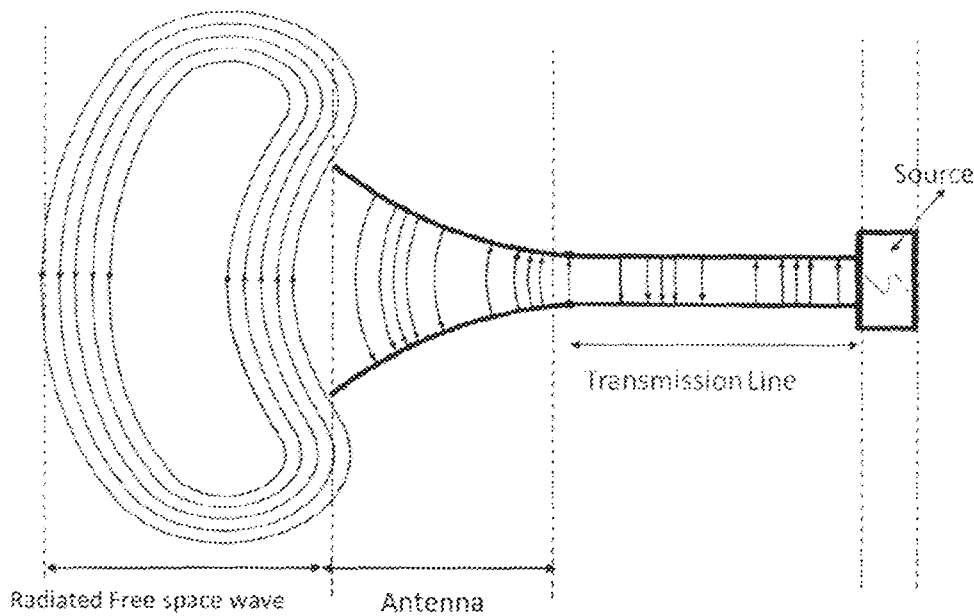


Fig 1.1: Antenna as a region of transition between guided wave and free space wave

Due to the time varying electric and magnetic fields, electromagnetic waves are created and these travel between the conductors. As these waves approach open space, free space waves are formed by connecting the open ends of the electric lines. Since the sinusoidal source continuously creates the electric disturbance, electromagnetic waves are created continuously; and, these travel through the transmission line, through the antenna and are radiated into free space. Inside the transmission line and the antenna, the electromagnetic waves are sustained due to the charges, but as soon as they enter free space, they form closed loops and are radiated.

1.1.2 Classification of Antennas

Antennas can be classified into five broad classes. These are electrically small antennas, resonant antennas, broadband antennas, aperture antennas and reflector antennas.

a. Electrically small antennas

There are various rules for considering an antenna to be electrically small. The most common criterion is that the largest dimension of the antenna (length, circumference) should be less than one-tenth of a wavelength. That is, $C < \lambda/10$, where C is the circumference and λ denotes the operating wavelength. Thus a dipole with a length less than $\lambda/10$, a loop with a diameter less than $\lambda/10$, or a patch with a diagonal dimension less than $\lambda/10$ would be considered electrically small (Kraus, 1988). These antennas have very low directivities and input impedance. They have high input reactance and low radiation efficiency.

Electrically small antennas are used at VHF frequencies and below. They are generally simple in structure and their properties are not sensitive to construction details. An important point regarding electrically small antennas is that their performance is closely related to their electrical size. The product of the bandwidth and the gain is a function of the size of the antenna, so that the gain can only be increased at the expense of the bandwidth and vice versa. Furthermore, an electrically small antenna is highly dependent on the environment in which the antenna operates, which must be taken into account.

The environment comprises both the device on which the antenna is mounted and the surroundings, mainly humans (Balanis, 2005). Electrically small antennas are not efficient

because of ohmic losses on the structure. They are commonly used in home and vehicle entertainment systems. An example is the vertical monopole used for reception in cars. Other examples are loop antennas and short monopoles (whip) for medium-wave (AM broadcast) reception.

b. Resonant Antennas

A resonant antenna is one that operates by means of a standing wave. Resonant antennas are often narrowband, because the optimum working frequency of the antenna depends on its dimensions. They operate well at a single or selected narrow frequency band so they naturally tend to prefer one frequency to the others (Carr, 2001). They are used from HF to S-Band frequencies. They have low gains and real input impedances. Types of resonant antenna include the monopole antenna, patch antennas and the dipole antenna.

c. Broadband Antennas

These antennas have acceptable pattern, gain and impedance that remain nearly constant over a wide frequency range. They are characterized by an active region with a circumference of one wavelength or an extent of a half wavelength which relocates with antenna frequency changes. For broadband antennas, the bandwidth is usually expressed as the ratio of the upper-to-lower frequencies of acceptable operation. For example, a 10:1 bandwidth indicates that the upper frequency is 10 times greater than the lower (Balanis, 2005). Properties include low to moderate but constant gain, real input impedance and wide bandwidth. They are mainly used from VHF to C-Band frequencies. Examples are helical antenna, spiral antenna and log periodic antenna.

d. Aperture Antennas

These can be defined as antennas that have an opening, called aperture through which propagating electromagnetic waves flow. The aperture is usually several wavelengths long in one or more dimensions. The radiation pattern usually has a narrow main beam, leading to high gain. The pattern narrows with increasing frequency thus increasing gain for a fixed physical aperture size. They are mainly used at UHF and above. Aperture antennas are very practical for space applications, because they can be flush-mounted on the surface of the spacecraft or aircraft (Balanis, 2005).

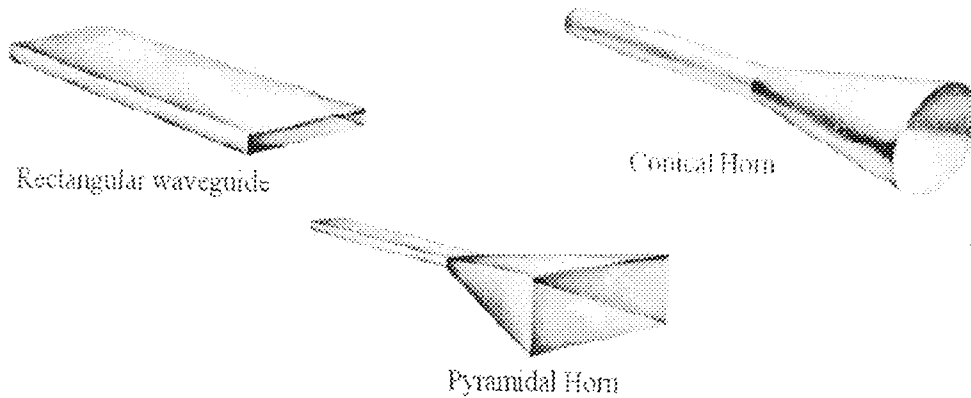


Fig 1.2: Examples of Aperture Antennas

The aperture can be covered with a dielectric material to protect them from environmental conditions. Horn antennas and parabolic reflector antennas are examples. Other examples are slits, slots, waveguides and lenses. Aperture antennas can also be designed for satellite applications where the beam-width can be used to determine the "footprint" area of the coverage.

e. Reflector Antennas

The need to communicate over great distances has led to the evolution of sophisticated forms of antennas with the ability to transmit and receive signals over millions of kilometers. Reflector antennas have large apertures. They can be described as secondary antennas used to amplify,

direct and shape the electromagnetic radiation emanating from primary antennas. The primary antenna in this case is usually referred to as feed antenna or simply "feed".

A very common antenna form for such an application is the parabolic reflector antenna. Antennas of this type have been built with diameters as large as 305 m (Balanis, 2005). Such large dimensions are needed to achieve the high gain required to transmit or receive signals after millions of miles of travel. Another form of a reflector, although not as common as the parabolic, is the corner reflector antenna.

1.1.3 Antenna Arrays

Major advances in millimeter wave antennas have been made in recent years. Usually the radiation pattern of a single element is relatively wide, and each element provides low values of directivity (gain). In many applications, it is necessary to design antennas with very directive characteristics (very high gains) to meet the demands of long distance communication. These specific radiation pattern requirements usually cannot be achieved by single antenna elements, because single elements usually have relatively wide radiation patterns and low values of directivity.

To design antennas with very large directivities, it is usually necessary to increase the electrical size of the antenna. This can be accomplished by enlarging the electrical dimensions of the chosen single element (Orfanidis, 2008). However, mechanical problems are usually associated with very large elements. An alternative way to achieve large directivities, without increasing the size of the individual elements, is to use multiple single elements to form an array.

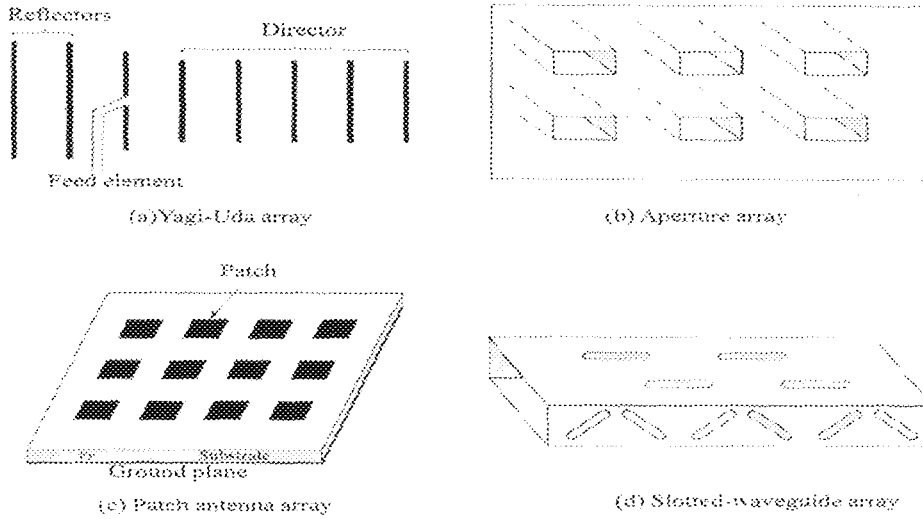


Fig 1.3: Typical wire, aperture, and Patch antenna array configurations (Balanis, 2005)

An array is a sampled version of a very large single element. In an array, the mechanical problems of large single elements are traded for the electrical problems associated with the feed networks of arrays (Balanis, 2005). Antenna arrays are used to direct radiated power towards a desired angular sector. The number, geometrical arrangement, and relative amplitudes and phases of the array elements depend on the angular pattern that must be achieved. Once an array has been designed to focus towards a particular direction, it becomes a simple matter to steer it towards some other direction by changing the relative phases of the array elements, a process called steering or scanning (Mirron, 2006).

1.2 Patch Antennas

In its most basic form, the patch antenna is a layer-structured antenna consisting of a very thin layer of metallic strip (patch) placed over a thin layer of dielectric substrate. On the other side (i.e. bottom) of the substrate is a conductive layer acting as a ground plane (Balanis, 2005). The patch is generally made of conducting material such as copper or gold and can take any possible shape.

The radiating patch and the feed lines are usually photo etched on the dielectric substrate. The length of the patch is usually chosen in the range $0.3333\lambda_0 < L < 0.5\lambda_0$ for a rectangular patch, where L is the length of the patch and λ_0 is the free-space wavelength. The patch is selected to be very thin such that the patch thickness $t \ll \lambda_0$. The height h of the dielectric substrate is usually chosen to be $0.003\lambda_0 \leq h \leq 0.05\lambda_0$ (Balanis, 2005). W is the width of the patch.

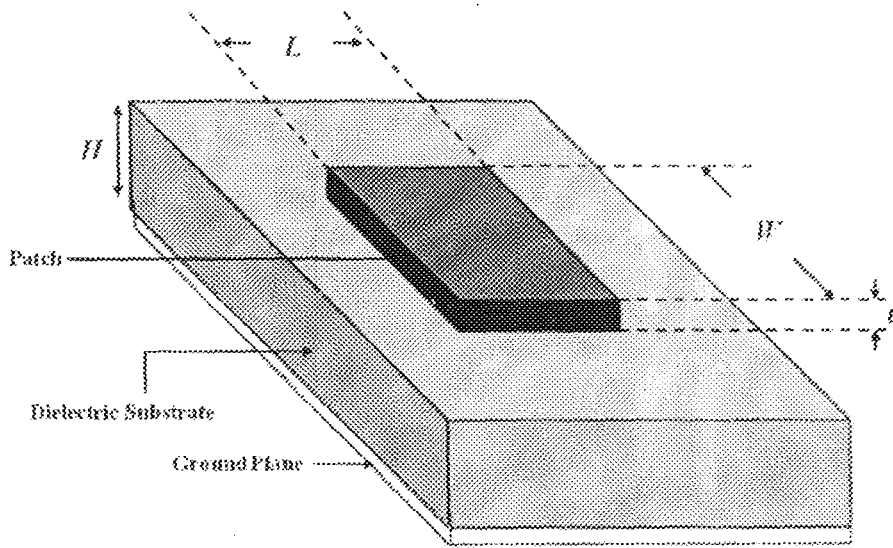


Fig 1.4: Basic patch antenna configuration

The substrate has a relative permittivity of ϵ_r , which is typically in the range $2.2 \leq \epsilon_r \leq 12$ (Balanis, 2005). The patch can be any shape, but the regular geometric shapes (such as rectangles or circular discs) are most commonly used.

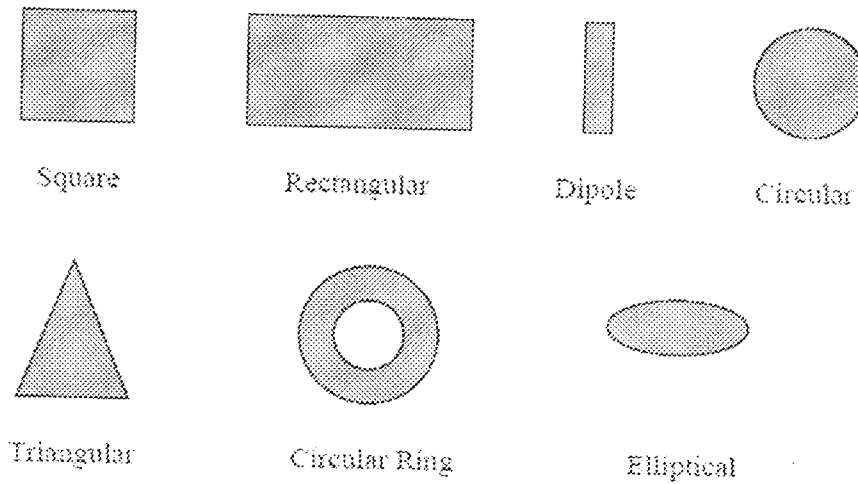


Fig 1.5: Common Shapes of patch Antennas

a. Advantages of Patch Antennas

Patch antennas are extensively utilized in present day wireless applications because of their low profile structure. This compact structure makes them greatly compatible for use in handheld devices like mobile phones, portable radios and pagers. They have been used successfully in satellite communication and also as communication antennas on board missiles because they can be manufactured to conform to the shape of the missile.

Some principal advantages of patch antennas are as follows (Kumar *et al*, 2003):

- a) Low profile planar configuration which can be easily made conformal to host surface.
- b) Low fabrication cost, hence can be manufactured in large quantities.
- c) Supports linear and circular polarization.
- d) Can be easily integrated with microwave integrated circuits (MICs).
- e) Light weight and low volume.
- f) Capable of dual and triple frequency operations.
- g) Mechanically robust when mounted on rigid surfaces

1.2.1 Patch Antenna Radiation Mechanism

The radiation of the patch antenna is determined from the field between the metal patch and the ground plane. Opposite charges are established on the bottom of patch and top of the ground plane when the patch is excited. While the attractive forces hold most of the charges between the two surfaces, the repulsive forces of the same charges on the patch surface will push some of the charges to the edges creating fringing fields which is the reason why patch antenna resonates (Garg *et al.*, 2001). The electric field is approximately constant along the width of the patch W and goes through a phase reversal along the length of the patch L (Balanis, 2005).

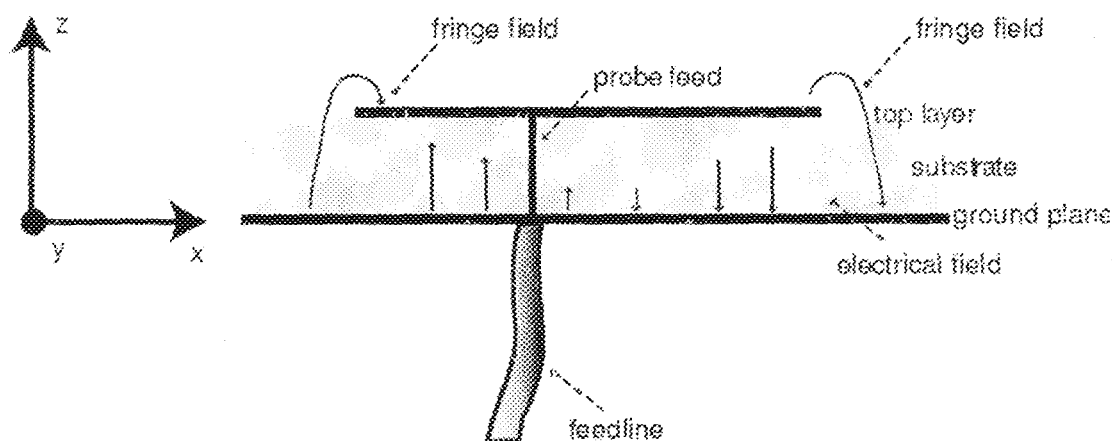


Fig 1.6: Patch antenna in its basic form showing electric field distribution (Orban and Moernaut, 2005)

1.2.2 Feeding Techniques for Patch Antennas

Patch antennas can be fed by a variety of methods, which can be classified into two categories: Contacting and Non-contacting feeding methods. In the Contacting method, the RF power is fed directly to the radiating patch using a connecting element such as a microstrip line. In the Non-contacting scheme, electromagnetic field coupling is done to transfer power between the microstrip line and the radiating patch (Balanis, 2005).

Four major feeding techniques have been identified. These are Microstrip line feed or Edge feed, Coaxial cable feed or Probe feed, Aperture coupled feed and Proximity coupled feed. The first two are contacting schemes whilst the last two are non-contacting schemes (Godara, 2002).

a. Edge Feed

In this type of feed technique, a conducting strip is connected directly to the edge of the patch. The conducting strip is smaller in width as compared to the patch. The purpose of the inset cut in the patch is to match the impedance of the feed line to the patch without the need for any additional matching element.

This is achieved by properly controlling the inset position. This is an easy feeding scheme, since it provides ease of fabrication and simplicity in modeling as well as impedance matching. This kind of feed arrangement has the advantage that the feed can be etched on the same substrate to provide a planar structure. However, as the thickness of the dielectric substrate being used increases, surface waves and spurious feed radiation also increases, which hampers the bandwidth of the antenna (Godara, 2002).

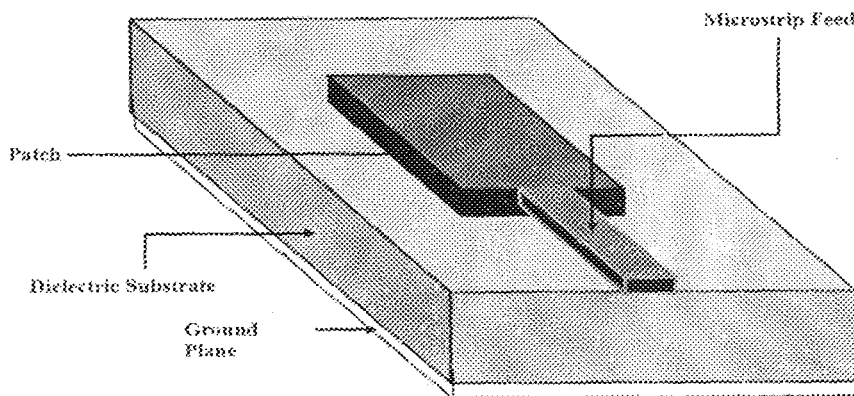


Fig 1.7: Edge feed for patch antenna

b. Probe feed

The coaxial feed or probe feed is a very common technique used for feeding patch antennas. In this technique, the inner conductor of the coaxial connector extends through the dielectric and is soldered to the radiating patch, while the outer conductor is connected to the ground plane. This technique is more complicated to actualize than the edge feed (Godara, 2002).

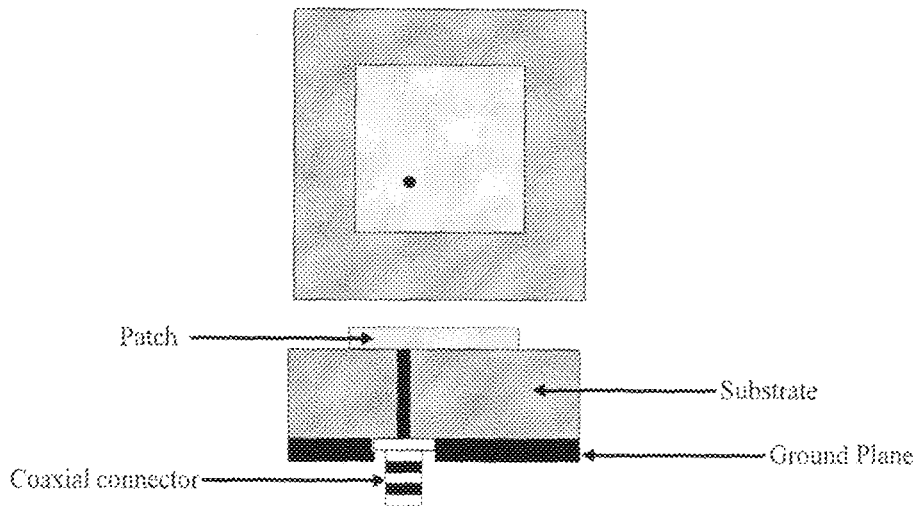


Fig 1.8: Probe feed for patch antenna

c. Aperture coupled feed

In this type of feed technique, the radiating patch and the microstrip feed line are separated by the ground plane. Coupling between the patch and the feed line is made through a slot or an aperture in the ground plane. The coupling aperture is usually centered under the patch, leading to lower cross-polarization due to symmetry of the configuration. Since the ground plane separates the patch and the feed line, spurious radiation is minimized. Unlike the probe-fed configuration, no vertical interconnects are required, simplifying the fabrication processes and also adhering to the conformal nature of printed circuit technology.

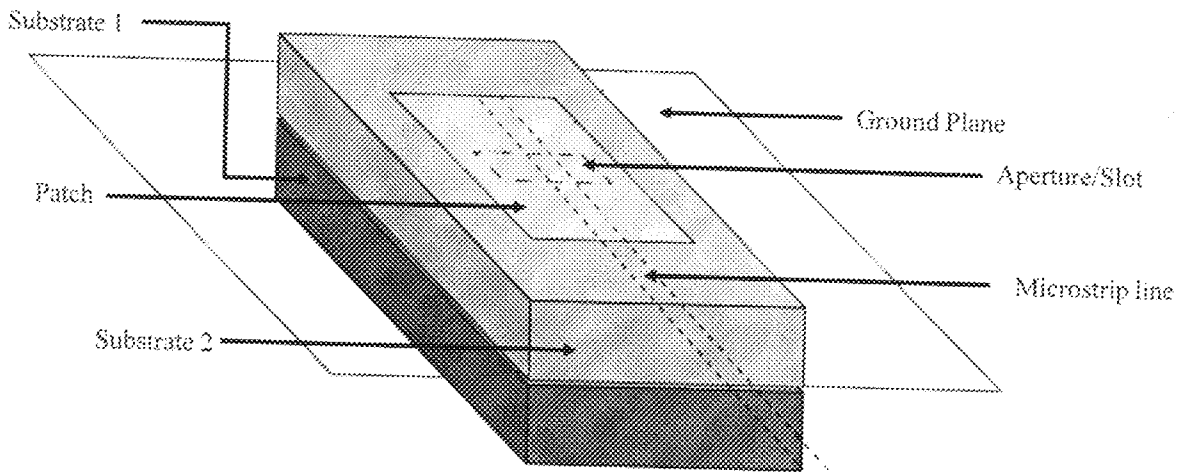


Fig 1.9: Aperture coupled feed for patch antenna

d. Proximity Coupled Feed

This is the second form of non-contact fed patches created to overcome the shortcomings of the direct contact fed patches (Pozar, 1987). In this scheme, two dielectric substrates are utilized in such a manner that the feed line is between the two substrates and the radiating patch is on top of the upper substrate. The main advantage of this feed technique is that it eliminates spurious feed radiation and provides very high bandwidth (as high as 13%) (Balanis, 2005).

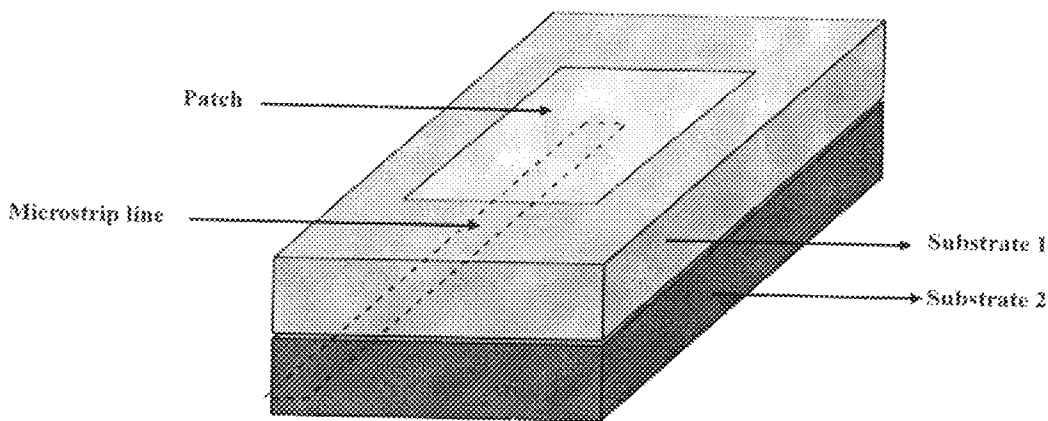


Fig 1.10: Proximity coupled feed for patch antenna

The major disadvantage of this feed scheme is that it is difficult to fabricate because of the two dielectric layers which need proper alignment. Also, there is an increase in the overall thickness of the antenna. The fact that there is no ground plane separating the two dielectric layers causes the power from the feed network to be coupled to the patch electromagnetically, as opposed to a direct contact. This is why this form of antenna is also referred to as an electromagnetically coupled patch antenna.

1.3 Patch Antenna Arrays

Parallel to the rising importance of wireless communication systems and personnel IT (Information Technology) services (e.g. Bluetooth), increasing efforts are devoted to the design and implementation of novel structures from miniaturized electronic circuits to the antenna arrays. One major area is the design of patch antenna arrays which are attractive candidates for adaptive systems in the present and future communication systems. In the past section, single patch antenna elements were discussed.

Usually the radiation pattern of a single element is relatively wide, and each element provides low values of directivity. Patch antenna array designs are optimized for the best radiation characteristics since the small size of patch antennas limits control of the pattern and one must use arrays of patches to control its pattern seriously (Milligan, 2005).

Their main advantages are light weight, low cost, planar or conformal layout, and ability of integration with electronic or signal processing circuitry. Patch antenna arrays can be classified based on their feed networks. There are two major types, namely; parallel-fed and series-fed

patch antenna arrays. Both types can be realized as either coplanar with the radiating elements or in a separate transmission line layer (Bahl and Bhartia, 2001).

1.3.1 Parallel-fed patch antenna arrays

These types of patch antenna arrays (also known as corporate fed) have a single input port and a multiple feed lines in parallel constituting the output ports. Each of these feed lines terminates at a patch antenna. Parallel fed patch antenna arrays are classified into two basic configurations. These are, one dimensional and two dimensional configurations (Bahl and Bhartia, 2001). Each of these configurations is hereby discussed.

a. One dimensional configuration

The one-dimensional parallel fed patch antenna array consists of a branching network of two-way power dividers. The total beam direction of the array can be controlled by manipulating the power division ratio at each junction. There are two basic configurations of one-dimensional parallel fed patch antenna arrays. These are symmetrical and asymmetrical configuration. The total number of patch antennas in the array is 2^n where n is an integer.

b. Two Dimensional configuration

The fundamental configuration of a two-dimensional parallel fed patch antenna array can be described as a one-dimensional array and its mirror image connected together as two sub-arrays of the same array. The basic sub-array configuration can be extended to larger arrays with specifically 2^n elements per side to maintain a symmetrical configuration.

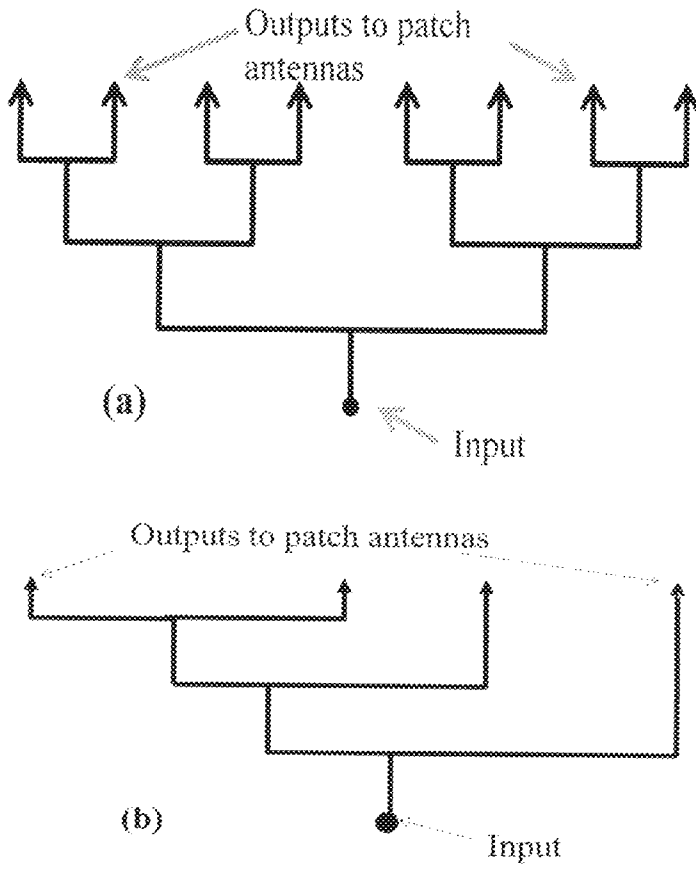


Fig 1.11: Basic one-dimensional parallel fed patch antenna array: (a) Symmetrical configuration.
 (b) Asymmetrical configuration

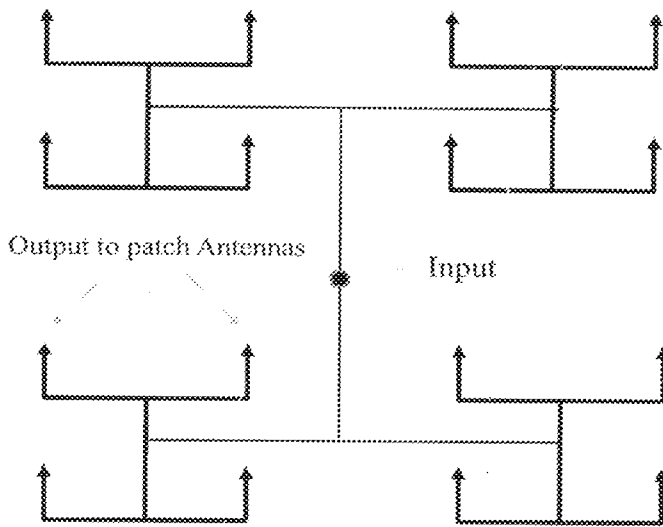


Fig 1.12: Two-dimensional parallel fed patch antenna array

1.3.2 Series fed patch antenna arrays

This type of patch antenna array has a continuous transmission line from which small proportions of energy are progressively coupled into the individual patch antennas distributed along the line by various means including proximity coupling, direct coupling, probe coupling and aperture coupling.

Typical series-fed microstrip patch antenna arrays can be configured into two types of radiating element arrangements. These are referred to as un-transposed and transposed arrays. Untransposed array has element spacing for the boresight beam of λ_g (free-space wavelength) whilst transposed array has a phase change of 180° on the radiated fields between adjacent elements due to the effects of the coupling mechanisms (Bahl and Bhartia, 2001)

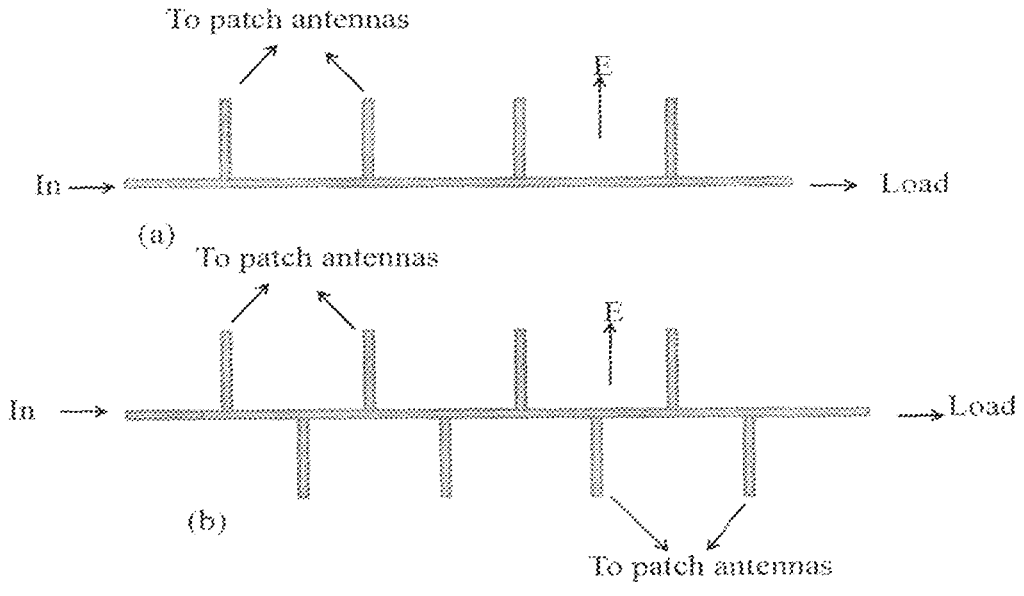


Fig 1.13: One-dimensional series-fed patch antenna arrays
(a) Untransposed configuration (b) Transposed configuration

The series fed patch antenna array constitutes a travelling wave array if the feed line is terminated in a matched load or a resonant array if the termination is an open or short circuit. In general the feed networks (parallel and serial) have a certain undesirable characteristics that must be carefully monitored in order to reduce any adverse effects on array performance. The characteristics include; Conductor and dielectric losses, Surface wave loss and spurious radiation due to discontinuities such as bends, junctions, and transitions. These losses constitute the overall insertion loss of the feed affecting the maximum obtainable gain of the array (Bahl and Bhartia, 2001).

1.4 Statement of the problem

A field of prominent economical and technological interest is that of wireless communications, especially satellite-based. Space-borne communication requires special care essentially due to the peculiar working environment (outer space). The antenna sub-system, in particular, must provide a wide coverage angle on the ground to cover, for example, Africa or the European Union, yet presenting a gain high enough to guarantee wide-band bi-directional communications.

Weight and dimensions must be as low as possible, on the satellite, where mass and size limitations are extremely strict. The antenna subsystems on majority of satellites, when fully deployed, utilize parabolic reflectors for their earthward beams. Over the past decades, the conventional feed for offset parabolic reflector antennas on-board satellites has been the horn, since they reduce the normally high E-plane side lobes and they provide the required directivity. One of the goals of the satellite antenna designer is to minimize the weight as much as possible without sacrificing the overall performance of the antenna.

The problem here is the weight of these horns. The horns tend to be bulky. Weight is a strong factor that affects cost of design and the overall cost of the launch campaign. High weight also increases the failure tendency in space missions. This research work therefore, is aimed at solving the weight problem constituted by conventional feed horns by proposing a patch antenna array as an alternative feed for dish antennas on board satellite.

1.5 Aims and Objectives

- a) To study the design, modeling methods and performance parameters of patch antenna arrays based on previous works.
- b) To design a patch antenna array that will operate in C-band
- c) To carry out a performance analysis on the designed array as feed for a dish antenna
- d) To tailor the patch antenna array feed in order to provide radiation characteristics similar to those of conventional feeds by varying the element spacing and excitation

1.6 Project Scope

This research work will introduce different types of antennas with emphasis on patch antenna elements and arrays. A review of papers related to patch antenna arrays and their applications will be carried out. This will be followed by the modeling and performance analysis of a patch antenna array as feed for C-band dish antenna. Simulation of patch antenna array feed for C-band dish will then be performed using the model developed. Conclusions will then be drawn and recommendations made based on the results. This research will however not consider the earth segment, which has no restriction on weight and maintenance.

CHAPTER TWO

2.0 LITERATURE REVIEW

2.0

2.1 Dish Antenna Feeding System and Aperture Efficiency

A dish antenna feeding system is positioned with its phase centre at the focus of the parabola so that the energy would radiate uniformly in all directions. Ideally, all the energy radiated by the feed will be intercepted by the parabola and reflected in the desired direction. To achieve maximum gain, this energy would be distributed such that the field distribution over the aperture is uniform. However, this is not practically realizable.

The most important property of the dish antenna that is considered as a measure of quality by the antenna engineer is the Aperture Efficiency. For a dish antenna, aperture efficiency (η_A) is defined as

$$\eta_A = A / A_g \quad (2.1)$$

Here A is the maximum absorption area and A_g is the geometrical area of the antenna aperture. It indicates the efficiency with which the radiation from a point source, for instance the transmitter on a communication satellite, is collected. It defines the sensitivity of the antenna. It is the product of a number of separate "efficiency components" (Baars, 2007).

$$\eta_A = \eta_i \eta_s \eta_r \eta_p \eta_e \eta_f \eta_b \quad (2.2)$$

where η_i = illumination efficiency of the aperture by the feed function ("taper")

η_s = Spillover efficiency of the feed (and sub reflector, if present)

η_r = Radiation efficiency of the reflector surface

η_p = Polarization efficiency of the feed-reflector combination

η_e = Surface error efficiency or scattering efficiency

η_f = Focus error efficiency (both lateral and axial defocus)

η_b = Blocking efficiency due to sub reflector or other obstruction.

2.1.1 Illumination taper

The most important component of the aperture efficiency is another basic quantity, the illumination efficiency. It describes the degree to which the outer areas of the aperture are less effectively exploited as a result of the "weaker" illumination of that area. When we look closely at the parabolic surface, we find out that the focus is rather far from the edge of the reflector than from the centre.

Since radiated power diminishes with the square of the distance (inverse square law) less energy arrives at the edge of the reflector than at the centre. This is referred to as space attenuation or space taper. Therefore to compensate for this, more power must be provided at the edge so as to have constant illumination over the surface of the reflector. Optimum performance is generally considered to be achieved with a -10 dB edge illumination taper (Wade, 2003).

2.1.2 Spillover

This is the percentage of power emitted by the feed, which "spills over" the edge of the reflector. The spillover efficiency is defined as the percentage of feed-radiated power which falls within the boundary of the reflector (Baars, 2007).

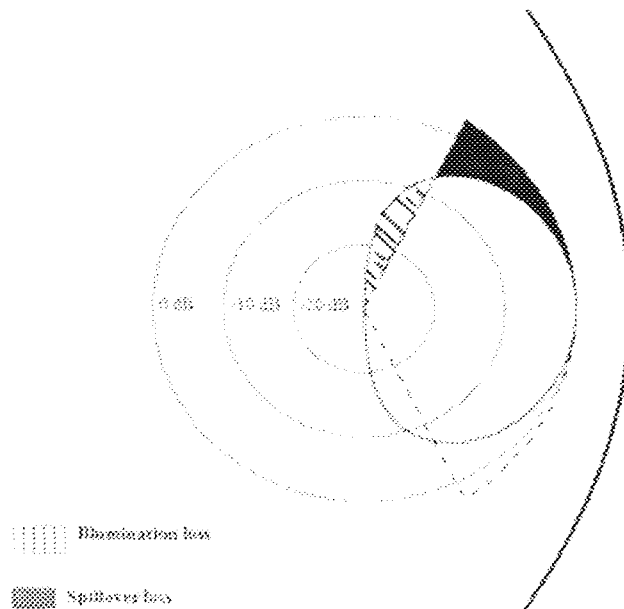


Fig. 2.1: Typical Dish illumination for a dish antenna

Illumination taper=10dB (Wade, 2003)

2.1.3 Surface errors

The small scale, randomly distributed deviations of the reflector from the prescribed parabolic shape result in randomly distributed phase errors over the aperture (Baars, 2007).

2.1.4 Focus

Axial or lateral displacements of the feed from the focus cause large scale phase errors over the aperture, which normally are amenable to calculation. These errors can be minimized by regular determination of the optimum focus from test observations (Baars, 2007).

2.1.5 Blocking

This is the partial shadowing of the dish aperture by the feed support structure. This leads to a loss of efficiency. The blocking area consists normally of two parts: the ‘plane wave blocking’,

equal to the projection of the structure onto the aperture plane, and the “spherical wave blocking”, which is the shadow cast by the spherical waves traveling from the outer region of the reflector outside the support penetration point to the focus (Baars, 2007).

2.1.6 The Cassegrain-feed

Cassegrain, a famous astronomer, showed that incident parallel rays can be focused to a point by utilizing two reflectors (Wade, 2003). To accomplish this, the main (primary) reflector must be a parabola, the secondary reflector (sub reflector) a hyperbola and the feed placed along the axis of the parabola usually at or near the vertex. A dish antenna with this type of feed arrangement is referred to as the Cassegrain antenna.

With the Cassegrain-feed arrangement, the transmitting or receiving equipment can be placed behind the primary reflector. This scheme makes the system relatively more accessible for servicing and adjustments (Balanis, 2005). This system requires a carefully shaped reflector which is more difficult to fabricate because a Cassegrain antenna must have a minimum diameter of 50 wavelengths with a reflector diameter of 20 wavelengths before the efficiency is higher than an equivalent dish with primary feed (Reasoner, 1989).

For this arrangement, the rays that emanate from the feed illuminate the sub-reflector and are reflected by it in the direction of the primary reflector, as if they originated at the focal point of the parabola (primary reflector). The rays are then reflected by the primary reflector and are converted to parallel rays, provided the primary reflector is a parabola and the subreflector is a hyperbola

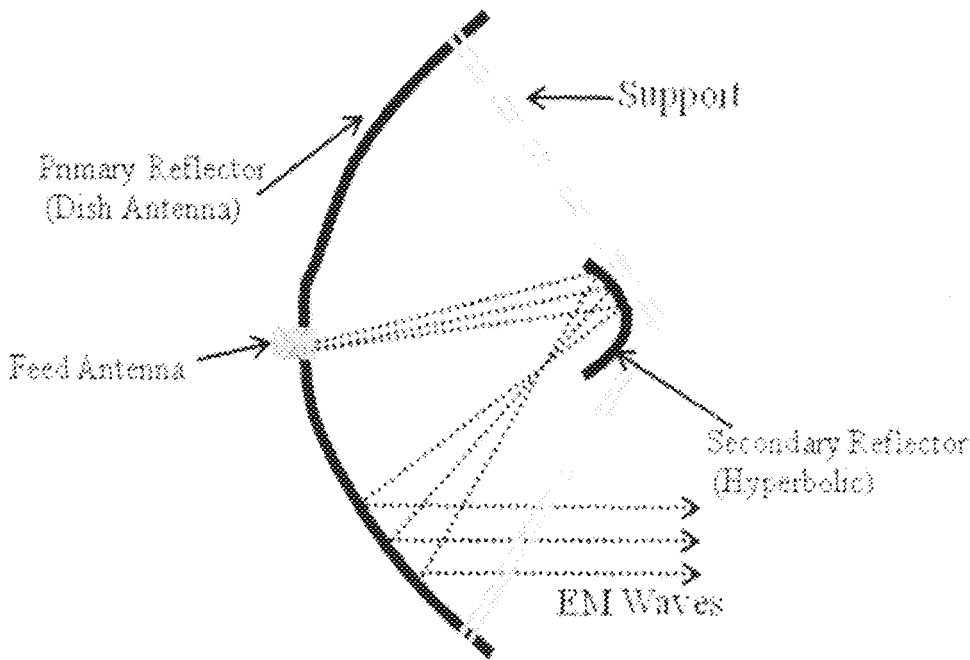


Fig. 2.2: Dish Antenna Cassegrain-feed arrangement

2.1.7 The F/D ratio

A common way to define a parabolic dish shape is with the F/D ratio, where F is the focal length and D the diameter of the dish: the smaller the ratio, the “deeper” the dish. Whatever the form, a parabolic dish can completely be specified with two parameters: The diameter D and the focal length F . Equivalently, the reflector antenna is specified in terms of D and the ratio F/D which gives the size, shape and curvature rate of the dish.

Typically, only measurement from the vertex to the rim is required, since a parabola of revolution consists of the same shape curve for all radial sections. F/D ratio is a convenient way to describe how much of a parabola is used (Wade, 2003).

2.2 Patch Antenna feed for a Parabolic Reflector

Michel (2004) of the Defence Research and Development of Canada (DRDC) designed a UHF circularly polarized patch antenna as a feed at 436 MHz for a 9.1 metre parabolic reflector. The feed was positioned at the focal point of the 9.1-metre parabolic reflector to establish a communication link with the first Canadian picosatellite, CanX-1, in the UHF-Band. The design was simple, inexpensive and done quickly. The patch antenna feed was chosen in order to achieve these objectives.

The feed consists of a patch antenna mounted on a 2 cm thick dielectric material over a finite ground plane. The circular polarization was obtained with two ports excited 90° out of phase. The realised feed exhibited the expected results in terms of input impedance. The 9.1 metre parabolic reflector has an F/D ratio of 0.36 corresponding to an aperture illumination of 140° . This meant that the patch antenna must provide a beamwidth of 140° .

Michel's first approach was to estimate the antenna dimensions using approximate equations. He made corrections to take into account the fringing field, based on the dielectric permittivity of the material, its thickness and the dimensions of the antenna. The physical length of the radiating patch is related to the different geometrical and electrical parameters by the following equations:

$$L_p = L - 2\Delta L \quad (2.3)$$

$$L = \frac{c}{2f_r \sqrt{\epsilon_{re}}} \quad (2.4)$$

$$\Delta L = 0.412h \frac{\epsilon_{re} + 0.3}{\epsilon_{re} - 0.258} \frac{W/h + 0.264}{W/h + 0.813} \quad (2.5)$$

where c is the velocity of light, f_r is the resonant frequency, ϵ_{re} is the effective dielectric permittivity, W is the patch width, h is the substrate thickness and ΔL is the fringe factor. At the time the study began, a centre frequency of 436 MHz was considered. As the operating frequency was approximately known, a relatively large impedance bandwidth was needed. An air-medium was first chosen to obtain the largest bandwidth.

As the bandwidth depends on the substrate height h , amongst other parameters, a large separation between the patch and the ground plane was chosen. A distance of 35 mm corresponding to 0.05 wavelength was considered. This led to a theoretical bandwidth of 14%. Using Equations (2.3) and (2.4), the physical length of the patch antenna was calculated to be 296 mm. This dimension was used as a starting point for optimizing the patch geometry with full wave simulation tools.

IE3D, a simulation software package from Zealand that is based on the method of moments, was used to optimize the antenna dimensions to obtain the best impedance matching at 436 MHz. The patch antenna, placed over an infinite ground plane was fed with a 50 Ω coaxial cable of 7 mm inner diameter. The optimization was then carried out with one port only to save computation time. Finally a 305 x 305 mm² patch placed at 35 mm above an infinite ground plane with the coaxial cable feed located 90 mm from the patch centre was chosen to obtain the best impedance matching.

The final design was simulated and the results of the simulation are presented in Figure 2.3. The figure shows a minimum value for the return loss at 435 MHz. It also indicates an impedance

bandwidth (-10dB points) from 428 MHz to 442 MHz (3.2% around a 435 MHz centre frequency). The coupling between the two ports is lower than -24 dB throughout the bandwidth.

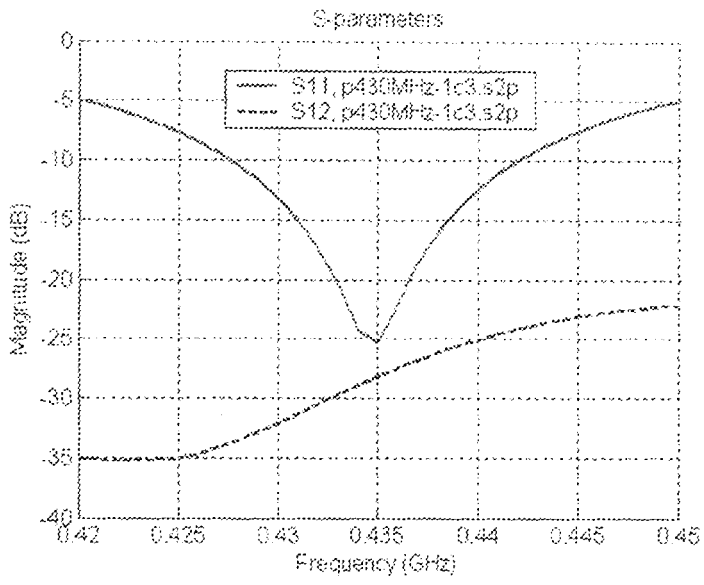


Fig 2.3: S-parameters of the patch antenna on air over an infinite ground plane (Michel, 2004)

2.3 Aperture Coupled Patch Antenna Array

Kuchar (1996) of the University of Technology, Vienna embarked on the design and implementation of a patch antenna array that meets the requirements of a base station antenna in a mobile communications system. The array needed no conventional beam forming network because it was meant to function as a digital controlled phased array. The array consists of nine linearly arranged single antennas with an element spacing of half a free space wavelength. The antenna was designed to operate in at 2.45 GHz, with a required bandwidth of 83.5 MHz

Aperture coupled feeding technique was implemented. This technique made it possible to use a low permittivity patch substrate with a large thickness to realize a broadband patch antenna. For the design of the antenna, **MultiStrip** and **Ensemble**, which are both simulation tools based on

the method of moments (MoM), were used. After optimizing and implementing a single element antenna that achieved satisfactory measurement results, the antenna array was worked out.

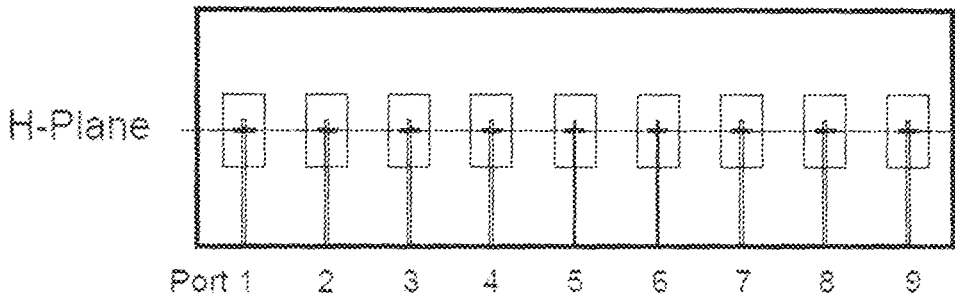


Fig 2.4: Top view of the 9-element antenna array (Kuchar, 1996)

Kuchar decided to implement an H-plane array since, with this configuration, no space problems due to the single feed lines arose. To identify each single antenna the elements have been numbered. He used a patch width in the order of $W_p \approx 0.2\lambda_0$. Then a distance of approximately $0.3\lambda_0$ remains between the non-radiating edges (See figure 2.5). MultiStrip was used for the simulations of a single element while Ensemble was used for the array simulations. To estimate the largest possible directivity of the nine-element array, an equiphased array was simulated using Ensemble and the result is presented in Figure 2.6.

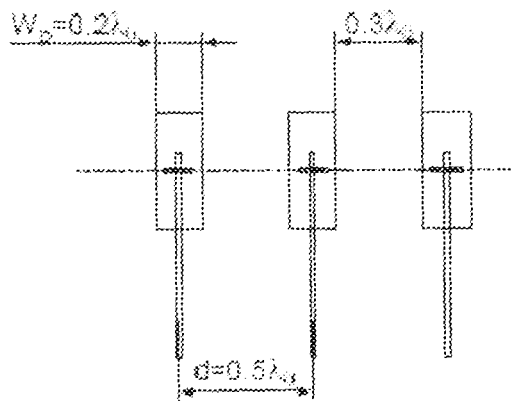


Fig 2.5: Array configurations for $0.2\lambda_0$ patch widths (Kuchar, 1996)

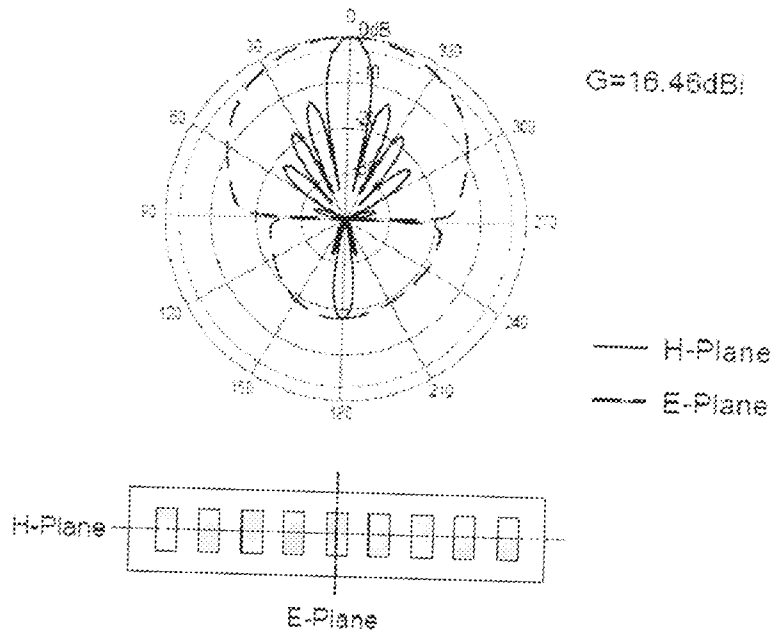


Fig 2.6: Simulated normalized power pattern for an equiphased nine element array (Kuchar, 1996)

Due to the H-plane array configuration, the E-plane pattern is the same as for the single element. The calculated maximum gain for the nine element array is $G = 16.46$ dBi.

2.4 Design of an 8X1 Square Patch Antenna Array

Anitha and Reddy (2009) designed an 8x1 patch antenna array for wind profiling radars operating in Doppler beam swinging mode. This was an attempt to provide an antenna with a narrow beam for wind direction accuracy. The antenna array was designed to operate in L-band with a linear configuration. In this design, coaxial feed was applied to a square patch antenna because it has an advantage that it occupies less space than the other feeds. The inner conductor of coaxial cable is connected to the radiating patch and the outer conductor is connected to the ground plane.

The first step in the design was to specify the dimensions of a single patch antenna. Here, Anitha and Reddy (2009) selected the half-wavelength rectangular patch element as the array element. The square-patch geometry is chosen since it can be arranged to produce circularly polarized waves. To meet the initial design requirements of 1.28 GHz operating frequency and 9° beamwidth, they based their calculations on the transmission line model (see equations (2.3), (2.4) and (2.5)). The dimensions of the square-shaped patch antenna element were specified from these approximate calculations.

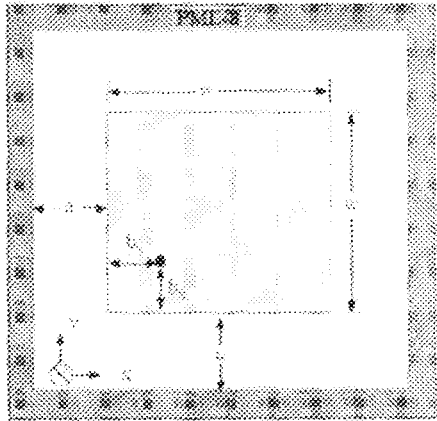


Fig. 2.7: The Square Patch Element (Anitha and Reddy, 2009)

For a linear array with a uniform excitation, the 3dB beam width (θ_{3dB}) is given by

$$\theta_{3dB} = \cos^{-1} \left[\sin(\theta_0) - 0.443 \frac{\lambda_0}{l} \right] - \cos^{-1} \left[\sin(\theta_0) + 0.443 \frac{\lambda_0}{l} \right] \quad (2.6)$$

where θ_0 is the main beam pointing angle, λ_0 is the free-space wavelength, and l is the total array length. The dimensions arrived at were $W = 7.6$ cm, $h = 3.175$ mm, $\epsilon_r = 2.2$ and $a = 9.5$ cm.

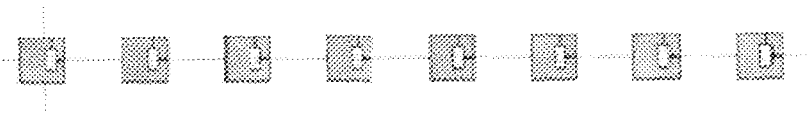


Fig 2.8: The 8X1 Array Configuration (Anitha and Reddy, 2009)

Anitha and Reddy then carried out simulations of the patch antenna array using IE3D software package. The results of the simulations showed that the patch antenna array exhibits a 20 MHz bandwidth, Voltage Standing Wave Ratio (VSWR) of less than 2 (same as for a single element) and the maximum gain reached 16.75 dBi at 1.28 GHz.

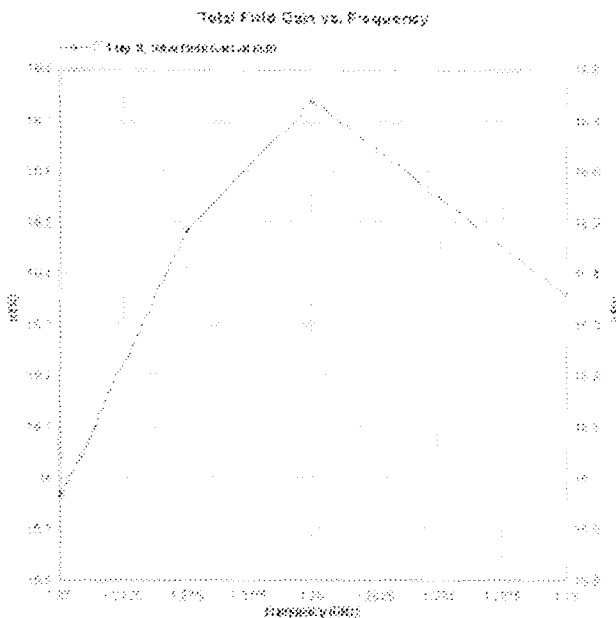


Fig 2.9: Gain Characteristics of an 8 element array (Anitha and Reddy, 2009)

Principal plane 2-dimensional radiation patterns at 1.28 GHz were computed for a single element and for the 8X1 linear array using IE3D software. When the inter-element distance was selected to be 0.73λ , the 8X1 array satisfies 9° beamwidth. The final array was then built by etching on a metalized dielectric substrate (RT/Duroid 5880). Gain, bandwidth and radiation patterns were computed for a frequency of 1.28 GHz. From the analysis of the data, it was also realized that the side-lobe level is the most critical factor and thus, determines the operating bandwidth.

2.5 Design, Simulation and Tests of a Low-cost Patch Antenna Array

Cakir and Sevgi (2005), embarked on the design simulation and testing of low cost patch antenna arrays. These arrays were designed to operate at 1.8 GHz band, with 35° beamwidths and 60° electronic scanning capabilities. The beamwidths are chosen because they are widely acceptable as standard for base station applications. These characteristics were required for complete cellular communication coverage of large cities like New York and in historical cities like Istanbul, where high buildings are separated by narrow but densely occupied streets.

The characteristics of these designed arrays were investigated using a Finite-Difference Time-Domain (FDTD) based and in-house prepared antenna simulation package called M-PATCH. The FDTD is chosen just because it is simple to implement, widely accepted, and very effective in visualization. Cakir and Sevgi also used the design to experimentally verify the effectiveness of, and to calibrate the simulation package (M-PATCH). The results of simulations and experiments agreed very well, and the arrays met the design criteria.

The designed antenna is a 3×3 array. The first step in the design was to specify the dimensions of a single patch antenna. Here, Cakir and Sevgi selected the half-wavelength rectangular patch element as the array element as commonly used in patch antennas. To meet the initial design requirements of 1.8 GHz operating frequency and 35° beamwidth, they based their calculations on the transmission line model. The length was specified by calculating the half-wavelength value and then subtracting a small length to take into account the fringing fields (see equations (2.3), (2.4) and (2.5)). The effective relative permittivity is given by

$$\epsilon_{re} = \frac{\epsilon_r + 1}{2} + \frac{\epsilon_r - 1}{2} \left(\frac{1}{\sqrt{1 + 12h/L}} \right), \quad (w/h \geq 1) \quad (2.7)$$

Using equation (2.6), Cakir and Sevgi evaluated the total array length to be $l \cong 23\text{cm}$ for 35° beamwidth. They then selected the inter-element distance to be half-wavelength. At this point, the 3×3 array was found to satisfy the 35° beamwidth on both planes normal to the patch surface. From these approximate calculations, the dimensions of the square-shaped patch antenna element were specified as $W = 5.52\text{ cm}$, $h = 1\text{ mm}$, $\epsilon_r = 2.2$ and $a = 2.758\text{ cm}$.

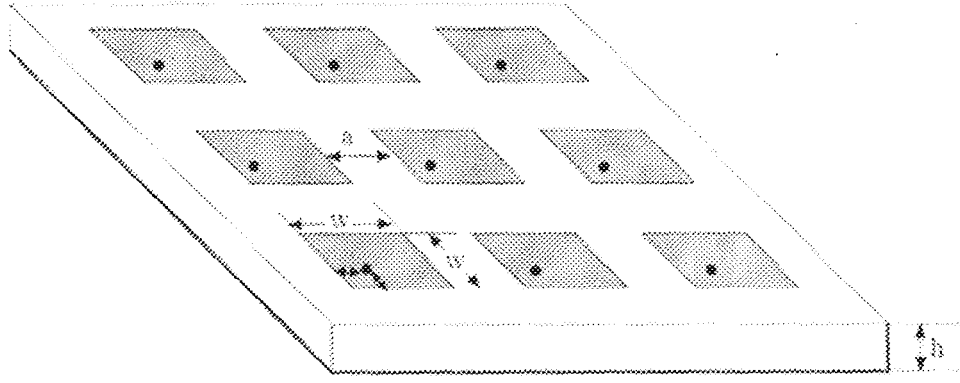


Fig. 2.10: The 3×3 patch array that operates at 1.8 GHz. and with 35° beamwidth
(Cakir and Sevgi, 2005)

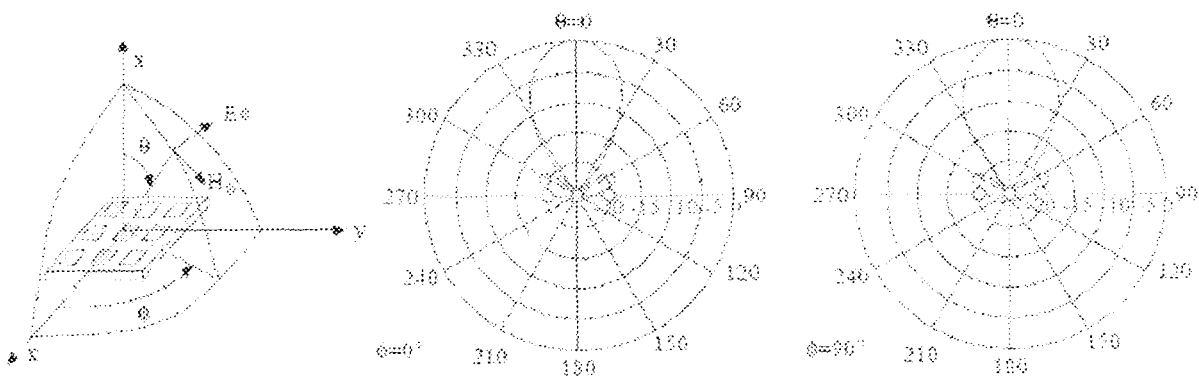


Fig. 2.11: Radiation patterns of the 3×3 patch at 1.8 GHz, left $\phi = 0^\circ$, right $\phi = 90^\circ$
(Cakir and Sevgi, 2005)

2.6 Genetic Algorithm Optimization for Circular Patch Antenna

Merad *et al* (2003) proposed the application of Genetic Algorithm (GA) to the optimization of a circular patch antenna. They emphasize the efficiency of this optimization algorithm when the goal is to find an approximate global maximum in high dimension, multi-modal function domain. They also stress that the GA method, is able to optimize different natural variables and is the most versatile approach to optimize the physical and electric parameters of the patch antenna. The concept of the Genetic Algorithm involves the use of optimization search strategies patterned after the Darwinian notion of natural selection and evolution.

During a GA optimization, a set of trial solutions is chosen and evolves toward an optimal solution under the selective pressure of the object function. Merad *et al* listed in their work the five basic tasks that a Genetic Algorithm optimizer must be able to perform as follows:

- a. Encode the solution parameters in the form of chromosomes
- b. Initialize a starting population
- c. Evaluate and assign fitness values to individuals in the population
- d. Perform reproduction using fitness weighted selection of individuals from the population
- e. Perform genetic operations to produce members of the next generation.

The genetic operations performed are listed in the following sub-paragraphs and represented by figure 2.12.

2.6.1 Selection and Reproduction

Each individual is selected using its fitness value. Reproduction is represented by the act of duplication of each individual based on the average of the performances for all the chromosomes

of population. Then individuals which give the best results have a good probability to be selected for the next generation.

2.6.2 Crossover

After reproduction we have crossover. This is a step where two randomly selected chromosome strings are each cut into two and their ends reversed and crossed to create two new chromosomes named children.

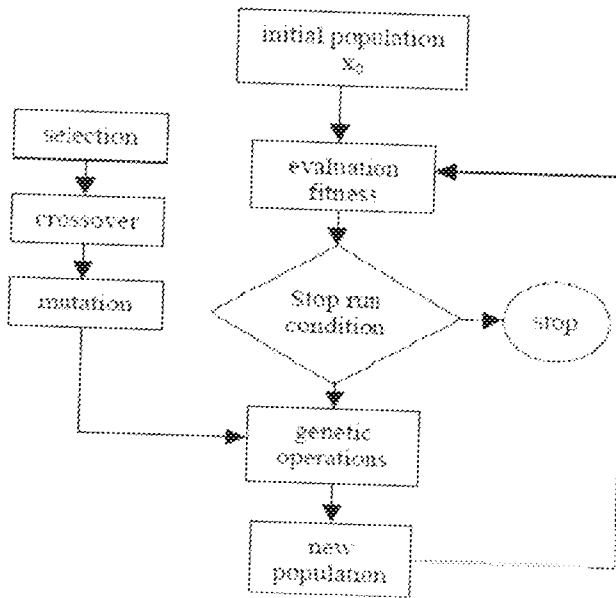


Fig. 2.12: Genetic Algorithm Process (Merad *et al.*, 2003)

2.6.3 Mutation

Mutation is a process whereby a bit value of a chromosome is modified randomly with a small probability (0.01- 0.1). A "1" becomes a "0" and a "0" becomes a "1". This is to mimic the natural theory of mutation according to Darwin. For the circular patch antenna in question, Merad *et al.* (2003) resolved to employ Genetic Algorithm to find the values of the three parameters: radius a , thickness H and ϵ_r , subject to the constraint of 5 GHz resonant frequency.

They employed equations 2.8 and 2.9 for resonant frequencies of TM_{nm} mode of a circular radiant element

$$f_{nm} = \frac{\alpha_{nm} c}{2\pi a_e \sqrt{\epsilon_r}} \quad (2.8)$$

$$a_e = a \left[1 + \frac{2H}{\pi a \epsilon_r} \left(\ln \frac{\pi a}{2H} + 1.7726 \right) \right]^{1/2} \quad (2.9)$$

Here α_{nm} represents the m^{th} zero of the derivative of the Bessel function of order n , c is the velocity of light in free space and a_e is the effective radius. Using the Genetic Algorithm context, Merad *et al* assimilates the antenna to a chromosome whose genes represent the parameters of this antenna (ϵ_r , H and a). In the first phase of the Genetic Algorithm process a population of individuals was created initially in a random way in the form of binary matrix.

This matrix contains a number $L \times C$ of figures 0 and 1 such that L , which is the number of lines, represents the number of individuals in the population and C , which is the number of columns, represents the number of parameters of the antenna multiplied by the number of bits of the simple binary code used. Each individual of the population was then evaluated by calculating the function of adaptation of each individual using the formula for gene decoding with N bits

$$P = \frac{P_{max} - P_{min}}{2^N} \sum_{i=0}^{N-1} 2^i b_i + P_{min} \quad (2.10)$$

where P_{max} and P_{min} represent the maximum and minimum ranges of the parameters and b_i are bit of order i along the gene corresponding to the parameter P . The vector P obtained was then introduced into the function f_{nm} to evaluate the fitness function of this individual. From this stage, new generations were created using the genetic operations mentioned earlier. The genetic characteristics employed are:

- a. Number of bits for coding of the parameters = 16
- b. Number of chromosomes by population = 100
- c. Number of generations = 20
- d. Probability of cross-over = 0.8 and Probability of mutation = 0.01

The results of optimization obtained are $\epsilon_r = 1.36$; $H = 0.35$ cm and $a = 1.25$ cm

Merad *et al* were able to successfully use genetic algorithm to determine the optimal parameters of a patch antenna, with circular radiant element and a coaxial probe feed. They concluded that the approach has the advantage of escaping the local solutions and it produced global optimal results without requiring a great deal of information about the solution domain. Figure 2.13 represents the evolution of the desired resonant frequency during the optimization phase.

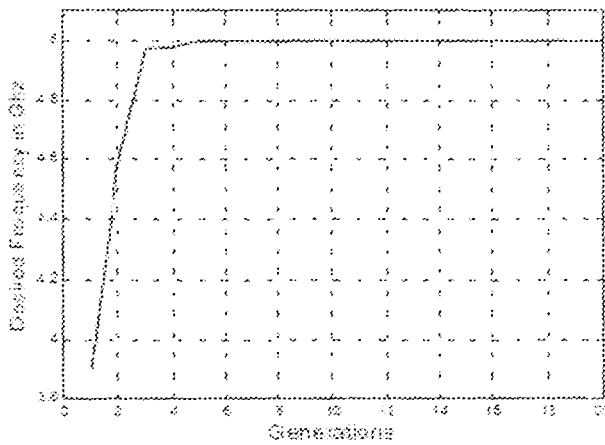


Fig. 2.13: Desired Frequency vs generations (Merad *et al*, 2003)

2.7 Design of patch antennas for satellite application

Erel (2002) of the Naval Postgraduate School Monterey, California embarked on the design and development of three-dimensional models for two patch antennas for installation on the NPSATI satellite. The patch antennas were to operate at 1.767 GHz and 2.207 GHz, for receiving and transmitting respectively. The antennas were designed with various constraints being considered.

The receive antenna is to operate with 187 MHz bandwidth while the transmit antenna is to operate with 310 MHz bandwidth. The Voltage Standing Wave Ratio (VSWR) of the two antennas should be 2:1 or lower. Input impedance must be 50Ω . Additional design requirements for the NPSAT1 satellite antennas also included strict dimension restrictions that the antenna dimension must not exceed 10 cm. This was based on the mission requirements.

To accomplish the thesis objective, the software utilized was CST Microwave Studio. This software was used to completely develop, test, and analyze the RF characteristics of the patch antennas and to determine the antenna parameters for optimal performance. The CST Microwave Studio is a specialized tool for fast and accurate three dimensional electromagnetic simulations of high frequency problems.

The design process included the electromagnetic modeling and simulation, which included obtaining port signals, the S-Parameter plots, and the far field pattern plots via CST Microwave Studio software (see figure 2.14).

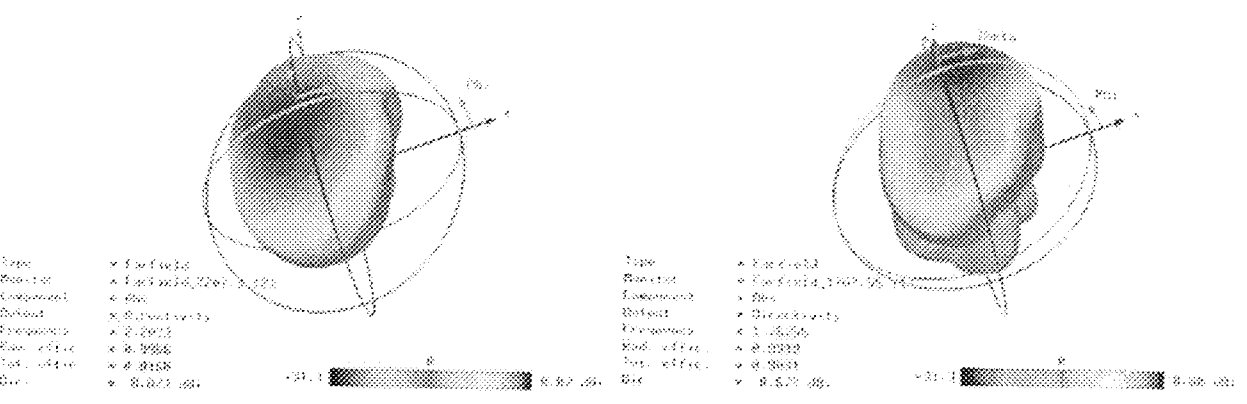


Fig. 2.14: 3-D Plot of Directivity for receive antenna (right) and transmit antenna (left) (Erel, 2002)

The simulation results showed that the proposed antennas satisfy the NPSAT1 requirements. Simulation results show that the maximum gain for the receive antenna was 8.6 dBi with side-lobe level of 11.6 dBi and the maximum gain for the transmit antenna was 8.8 dBi with side-lobe suppression of 15.7 dBi. The Department of Defense (DOD) then proceeded on the implementation of these antennas based on these acceptable results.

2.8 Cylindrical Patch Antenna Array

Keskilammi and Kivikoski (2007) of the Tampere University of Technology, Finland proposed a three-element cylindrical antenna array for 2.45 GHz Radio Frequency Identification (RFID) applications. Radio Frequency Identification consists of three components: a transponder or tag that is attached to the item to be identified, a reader or scanner that communicates with the tag using radio frequency signals and a host data processing system that contains the information of the identified item and distributes the information between other remote data processing systems. For the tag, an omni-directional antenna is preferred to ensure identification from all directions.

The dipole antenna is employed in most cases but it has the shortcoming that it cannot be attached straight on metal objects. So for metal tags, patch antennas are the preferred option. Keskilammi and Kivikoski (2007) thus proposed a cylindrical patch antenna array as a solution to this. They suggested that omni-directionality can be achieved using the antenna array which can be wrapped around the metal object or the metal object itself can be used as a ground plane for the antenna. They embarked on the modeling and simulation of the antenna array using software based on finite element method (FEM).

The substrate material employed in the modeling was a double-sided flexible PCB, having thickness of 0.236 mm. The dielectric constant of the substrate was $\epsilon_r = 3.32$. The conductive material in the model was 35.0 μm thick copper. Three square patch elements were equally placed on cylinder surface. The three coaxial feed points were located 120° apart on the cylinder. The diameter of the cylinder was $\phi = 67.0$ mm and the height was $h = 100.0$ mm. The size of the patch element was 33.0mm x 33.0mm. Inside of the cylinder was a continuous ground plane.

The antenna array was fabricated along the dimensions from the model of the simulation software on a flexible PCB. The 3D view of the 3-element cylindrical patch antenna array obtained using the simulation software is shown in figure 2.15.

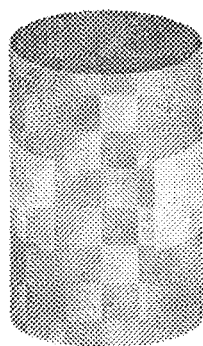


Fig. 2.15: 3D View of a 3-element array taken from the simulation software

(Keskilammi and Kivikoski, 2007)

The resonant frequencies of the elements are 2.45 GHz, 2.46 GHz and 2.47 GHz. The S-parameters and the radiation pattern of the antenna array were measured in an electromagnetically anechoic antenna measurement laboratory for three operation modes. The measured values were observed to compare favorably with the simulations.

2.9 Circular Patch Antenna Array for C-Band

Keshikar *et al* (2008) embarked on the design, construction and test of an array of circular patch antennas. The antenna was designed to be used in altimeter system applications, in the C-band. The aim of this antenna construction was to obtain a gain of 12 dB, an acceptable pattern, and a reasonable value of Voltage Standing Wave Ratio (VSWR). The selected antenna here is a patch antenna array consisting of four equal circular elements with equal spacing, placed in the H-plane. The antenna array is fed from its centre.

The first step in the design was to specify the dimensions of a single patch antenna. The cavity model was applied to analyze the patch. For patch design, it was assumed that the dielectric constant of the substrate (ϵ_r), the resonant frequency (f_r), and the height of the substrate h are known. The dimensions of the single circular patch antenna were obtained by choosing

$$f_r = 4.3\text{GHz}, \quad h = 0.16 \text{ cm}, \quad \epsilon_r = 2.33$$

and substituting these values in equation (2.8) to obtain the patch radius $a = 1.25\text{cm}$.

Keshikar *et al* then employed Ansoft Ensemble 8 software that is based on the method of moments to simulate the circular patch antenna array. The spacing (S) = d arrived at between the array elements is 3.8 cm. The selected array is a 4x1 patch antenna array ($N=4$) with equal spacing and uniform excitation. The beam patterns for this antenna array were estimated using the following equations.

$$BWFN = 2 \frac{\sqrt{2\lambda}}{Nd} = 2 \frac{\sqrt{2 \times 7 \times 10^{-2}}}{4 \times 3.8 \times 10^{-2}} = 115^\circ \quad (2.11)$$

$$HPBW = 2 \sqrt{0.866 \frac{\lambda}{Nd}} = 2 \sqrt{0.866 \frac{7 \times 10^{-2}}{4 \times 3.8 \times 10^{-2}}} = 76^\circ \quad (2.12)$$

BWFN is the beam width between first nulls and *HPBW* is the half-power-beam width. The designed antenna was then completely analyzed using commercial HP High Frequency Structure Simulator (HPHFSS) software. From the simulations a directivity of 13 dB at 4.3 GHz was achieved with the main lobe in the broadside direction, with the 50-degree HPBW, and 25dB SLL (ratio of the maximum value of the largest side lobe to the maximum value of main lobe). The pattern is almost symmetric (in both E-plane and H-plane), and the side lobes are very small (see Figure 2.16).

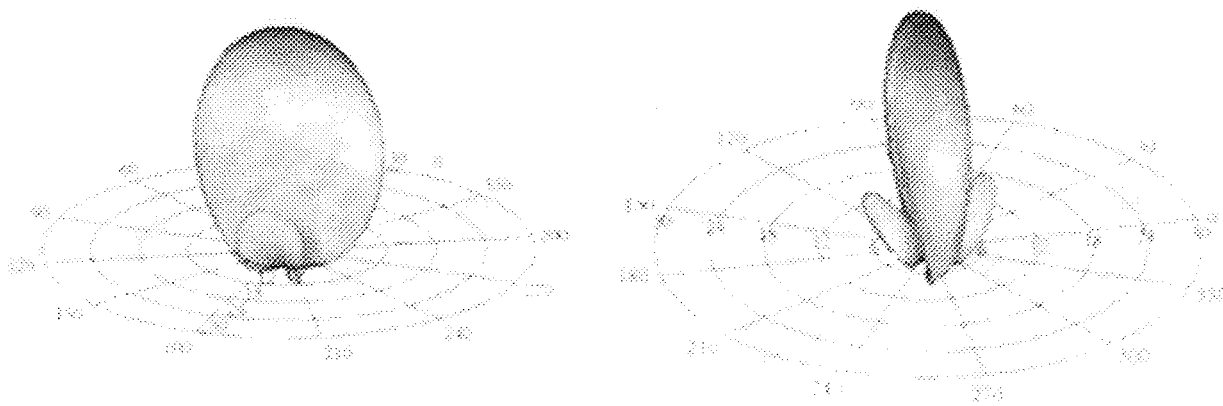


Fig. 2.16: Three-dimensional pattern of the patch antenna array $\phi=0^\circ$ and $\phi=90^\circ$ simulated with the HPHFSS 5.4 (Keshtkar *et al*, 2008)

The array antenna was then fabricated using the designed values. An inset feed scheme was employed to match the patch antenna to a 50 Ω coaxial probe feed. The dielectric material has a permittivity of 2.33 and a thickness of 0.16 cm. The substrate of this antenna is made of RT/Duroid 5870. Tests and measurements were carried out on the patch antenna array. In the test process, the antenna pattern and the value of VSWR were obtained. The geometry of the circular patch antenna array is shown in figure 2.17.

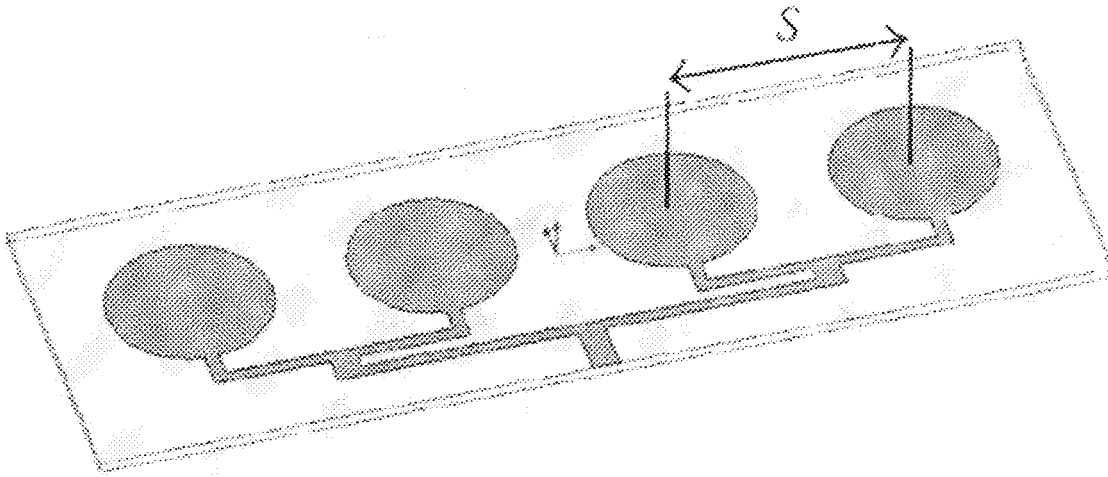


Fig. 2.17: Geometry of the array of circular patch elements (Keshtkar *et al.*, 2008)

Antenna radiation performance was measured and recorded in two orthogonal principal planes (E-plane and H-plane). Results of the measurements show that the designed antenna exhibits good performance in terms of return loss and radiation. Good agreement was obtained between simulation and experimental results, providing validation of the design procedure.

2.10 Circular Patch Array Antenna for KU-band

Lai *et al* (2008) proposed a 36 - element circular patch antenna array to operate in Ku-band as an alternative to the parabolic dish for satellite communications. Till date the dish is known to provide the best gain, which is about 37 dB at 12.5 GHz for 0.6 m diameter, 38.5 dB for 0.75 m and 40.3 dB for 0.9 m. The patch antenna array performance in this band was found to be able to compare favorably with the dish performance and it also has its inherent advantages such as small dimensions, light weight, slim size and easy manufacturing to go along with this.

As usual the first step was the design of a single element. It then developed into 36 elements in a 6X6 array configuration. Finally, Advance Design System (ADS) software was used to compute

the gain, power, radiation pattern, and S- parameters of the antenna. In this array antenna, each element is connected by a microstrip line which transforms the impedance of the patch into 50Ω .

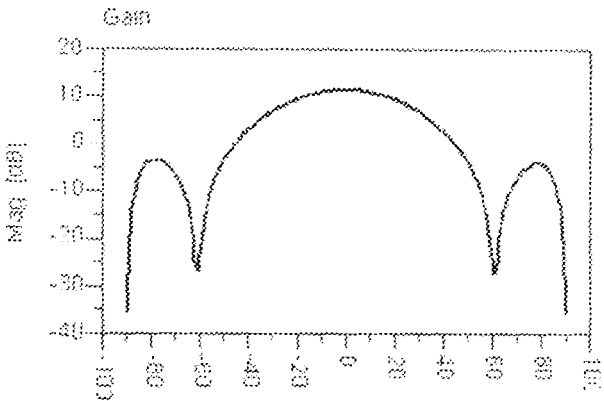


Fig. 2.18: The Simulated Gain of the circular patch array antenna (Lai *et al*, 2008)

The patch antenna array is corporate fed (see section 1.3.1) with each element connected to the feed transmission lines. With this method, more control can be actualized on the feed of each element (amplitude and phase) and this is ideal for scanning phased arrays, multi-beam arrays, or shaped-beam arrays.

All the results simulated were the optimum values which were generated by ADS. Though the antenna was designed to operate at 15 GHz, from the simulation results, the antenna got resonance at 18 GHz. Lai *et al* suggested that the gain can be improved by increasing the number of elements. The gain of the antenna was simulated to be 10 dB in 0° direction. It is also seen that the Circular Patch Array Antenna has very narrow bandwidth.

2.11 Design of a Circularly Polarized Patch Array

Alatan (2002) of the Electrical & Electronics Engineering Department, Middle East Technical University, Ankara embarked on the design of a series-fed circularly polarized patch array that is to operate in S-band. This antenna array was to be used as a sub-array for a ground-based

antenna receiving signals from a LEO (Low Earth Orbit) satellite. A square patch antenna was chosen as the array element and the circular polarization operation is obtained by feeding the antenna with two slots placed orthogonal to each other and excited with a 90° phase shift. The end of the feed line is terminated with a matched load to improve the bandwidth of the antenna.

First, a single slot-coupled square patch antenna operating at 2.21 GHz was designed by using Ensemble, an Electromagnetic Simulation Software by Ansoft. The dielectric constant and thickness of the substrates for the feed line layer and the patch layer are chosen as

$$\epsilon_r(\text{feedline}) = 3.48, d(\text{feedline}) = 0.76 \text{ mm}, \epsilon_r(\text{patch}) = 3.48, d(\text{patch}) = 1.52 \text{ mm},$$

respectively. The width of the 50 Ω transmission line was calculated to be 1.72 mm.

To obtain the resonance frequency of the antenna at 2.21 GHz, the dimensions of the square patch and the coupling slot are found as

$$L(\text{patch}) = W(\text{patch}) = 35.23 \text{ mm and } L(\text{coupling}) = W(\text{coupling}) = 1.5 \text{ mm}$$

After achieving a successful design of a single antenna, Alatan selected a series fed 8-element antenna array configuration for the design. All the antenna elements are fed in-phase to obtain broadside radiation. Ensemble Software was used to develop, test, and analyze the RF characteristics of the patch antennas and to determine the antenna parameters for optimal performance. Simulations revealed that a wide input impedance bandwidth was obtained for the 8-element series fed Circularly Polarized Patch Array.

From The simulated radiation pattern plot at 2.21 GHz, Alatan discovered that Right Hand Circular Polarization (RHCP) operation was maintained for the 8-element array design with a cross polarization rejection ratio of -25dB. The lengths of the feed lines between successive slots are also adjusted successfully so that the array provides broadside radiation. The radiation

patterns were calculated at $2.21\text{GHz} \pm 10\text{ MHz}$ and it was observed that circular polarization operation was preserved within the 20 MHz bandwidth. The simulation results obtained by Ensemble, implies that the design goals are achieved.

In order to achieve maximum gain and maximum efficiency, illumination loss should be eliminated. This means that energy from the feed should be distributed uniformly over the aperture of the dish antenna (Wade, 2003). So, more energy is required at the dish edges than at the center because the edges are farther to the feed location than the centre. This should also be achieved without any energy missing the reflector to eliminate spillover loss. This is not practically realizable using conventional feeds like the horn.

From the reviewed works, we acknowledge the fact that the beam pattern of patch antenna arrays can be tailored to provide a desired gain (Keshkar *et al.* 2008). They can be shaped to give us a desired beam width (Cakir and Sevgi, 2005). They can even be designed to comply with stringent dimension restrictions (Erel, 2002). In this thesis, a C-Band patch antenna array feed is designed for a dish antenna starting from the design of a single patch array element.

Attempts are made to tailor the patch antenna array feed to provide radiation characteristics that will lead to perfect illumination, maximum gain and maximum efficiency by varying the element spacing and excitation. This is done using Genetic algorithm optimization technique on MATLAB platform. The RF characteristics of the designed array are then completely analyzed using PCAAD 5.0 and MATLAB.

CHAPTER THREE

3.0 MATERIALS AND METHODS

3.1 The single patch antenna array element

The first step in the design of a patch antenna array is to specify the dimensions of a single patch antenna. The patch antenna can be of any shape. The aim is to choose a simple geometry for the patch antenna. This is to simplify the analysis and performance prediction. So here, the circular patch antenna is chosen as the array element. Its characteristic parameters are the radius a , and thickness h as shown in figure 3.1.

The most popular models for the analysis of patch antennas are the transmission line model, cavity model, and full wave model (Balanis, 2005). The transmission line model is the simplest of all and it gives good physical insight but it is less accurate. The cavity model is more accurate and gives good physical insight but is complex in nature. The full wave models are extremely accurate and versatile but are far more complex in nature. In this project, the cavity model is applied to analyze the circular patch antenna array element.

There are three essential parameters required for the design of a circular Patch Antenna. These are: Frequency of operation (f), Dielectric constant of the substrate (ϵ_r), and Height of dielectric substrate (h):

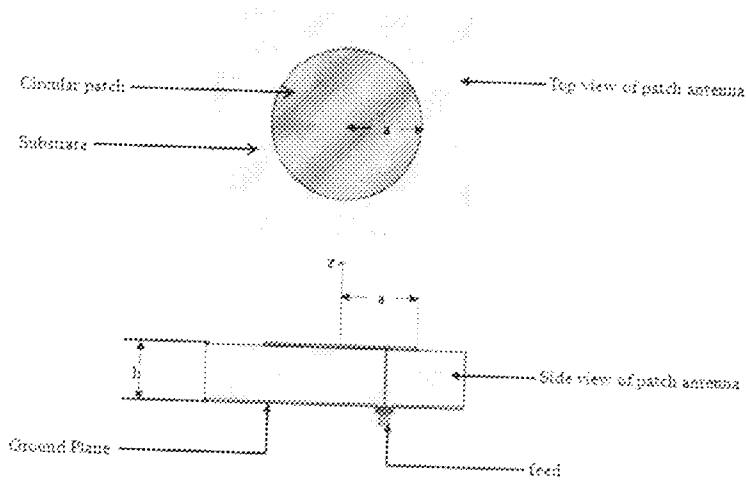


Fig 3.1: The single circular patch antenna element, $a = 0.88$ cm

a. Frequency of operation f

The resonant frequency of the antenna must be selected appropriately. The antenna is to be used for satellite communications in the C-Band frequency range that is 4-8 GHz. Therefore a resonant frequency of 6.0 GHz is selected for the purpose of this work.

b. Dielectric constant of the substrate ϵ_r

For the patch antenna to be part of a satellite payload, it is essential that the antenna is not bulky. This is the primary consideration in the choice of the substrate. The substrate selected for this antenna is made of RT/Duroid 5870 from Rogers Corporation. This material has a relative permittivity of 2.33. It also has heritage in the space industry.

c. Height of dielectric substrate h

To minimize losses and maximize the radiation efficiency of a patch antenna, the thickness of substrate must satisfy the relation (Garg *et al.*, 2001)

$$\frac{h}{\lambda} \leq \frac{0.3}{2\pi\sqrt{\epsilon_r}} \tag{3.1}$$

Substituting values for λ and \mathcal{E}_r in equation (3.1) we have

$$h \leq \frac{0.3 \times 5}{2\pi\sqrt{2.33}} \quad (3.2)$$

That is,

$$h \leq 1.6 \text{ mm}$$

Thus the height h of the dielectric substrate is selected as 1.6 mm for this design purpose.

Hence, the essential parameters for the design are:

Frequency of operation, $f = 6.0$ GHz

Dielectric constant of the substrate, $\mathcal{E}_r = 2.33$

Height of dielectric substrate, $h = 1.6$ mm

The physical radius a , of the circular patch antenna is given by the expression (Balanis, 2005).

$$a = \frac{F'}{\left\{1 + \frac{2h}{\pi\mathcal{E}_r F'} \left[\ln\left(\frac{\pi F'}{2h}\right) + 1.7726 \right] \right\}^{\frac{1}{2}}} \quad (3.3)$$

where

$$F' = \frac{8.791 \times 10^9}{f\sqrt{\mathcal{E}_r}} \quad (3.4)$$

and h is in centimeters

Substituting values, for the parameters,

$$F' = \frac{8.791 \times 10^9}{6 \times 10^9 \sqrt{2.33}} = 0.9599 \quad (3.5)$$

Therefore, the physical radius is

$$a = \frac{0.9599}{\left\{1 + \frac{2 \times 0.16}{\pi \times 2.33 \times 0.9599} \left[\ln\left(\frac{\pi \times 0.9599}{2 \times 0.16}\right) + 1.7726 \right] \right\}^{\frac{1}{2}}} \quad (3.6)$$

$$= 0.8825$$

Thus, the estimated physical radius of the single circular patch antenna element $a \cong 0.88$ cm

3.2 The Dish Antenna

Before we proceed on the design of the patch antenna array, we have to select the dish antenna. The dish antenna selection for the purpose of this work is based on the F/D ratio (see section 2.1.7). Most commercial microwave antennas use an F/D ratio of 0.25 to 0.38, with 0.32 to 0.36 the most common (Singer, 2003).

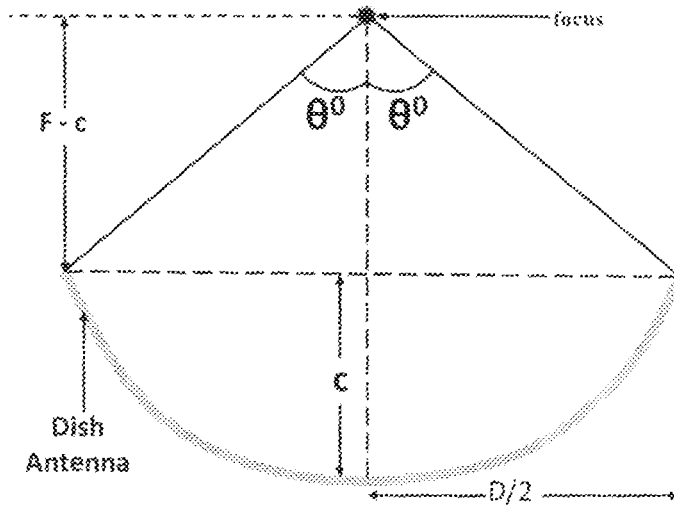


Fig 3.2: Basic dish antenna geometry

Thus an F/D ratio of 0.36 is selected. From basic dish antenna geometry (figure 3.2), the focal distance F is related to the diameter D of the dish by (Pietrosemoli, 2004)

$$F = \frac{D^2}{16 \times c} \quad (3.7)$$

where c is the depth of the parabola at its center. Also we observe that 2θ is the total angle subtended by the dish at its focus. This represents the dish aperture illumination. From the geometry,

$$\tan \theta = \left[\frac{\left(\frac{D}{2}\right)}{F - c} \right] \quad (3.8)$$

Substituting the values and expanding the equation, we have

$$\text{Aperture Illumination} = 2 \tan^{-1} \left[\frac{8 \left(\frac{F}{D} \right)}{16 \left(\frac{F}{D} \right)^2 - 1} \right] \quad (3.9)$$

Therefore, it can be deduced that the aperture illumination of any dish is only determined by its F/D ratio and the relationship is given in equation (3.9). Therefore, substituting the values,

$$\text{Aperture Illumination} = 2 \tan^{-1} \left[\frac{8 \times 0.36}{16 \times (0.36)^2 - 1} \right] \cong 140^\circ \quad (3.10)$$

This means that the selected F/D ratio of 0.36 corresponds to an aperture illumination of 140° .

3.3 The patch antenna array feed design

For a dish antenna, feed selection should be done in such a manner that the feed achieves a compromise of illumination loss and spillover loss which yields maximum performance. The traditional rule of the thumb for this compromise is that the best efficiency occurs when the illumination energy is 10 dB down at the edge of the dish (Wade, 2003). In order to replace conventional feeds by a patch antenna array, it is important that the array provides similar radiation pattern to the conventional feeds (i.e. up to -10 dB beamwidth).

In this work, two approaches will be considered in solving this problem. The first approach is to attempt to eliminate illumination loss and maximize gain. Therefore, for the dish antenna with F/D of 0.36, the patch antenna array feed must provide a beam with radiation pattern such that the first null beamwidth (FNBW) is 140° . As discussed earlier, the aim is to maintain a simple geometry and configuration for the patch antenna array. Thus an 8x1 linear array configuration (see figure 3.3) is selected with a broadside radiation pattern.

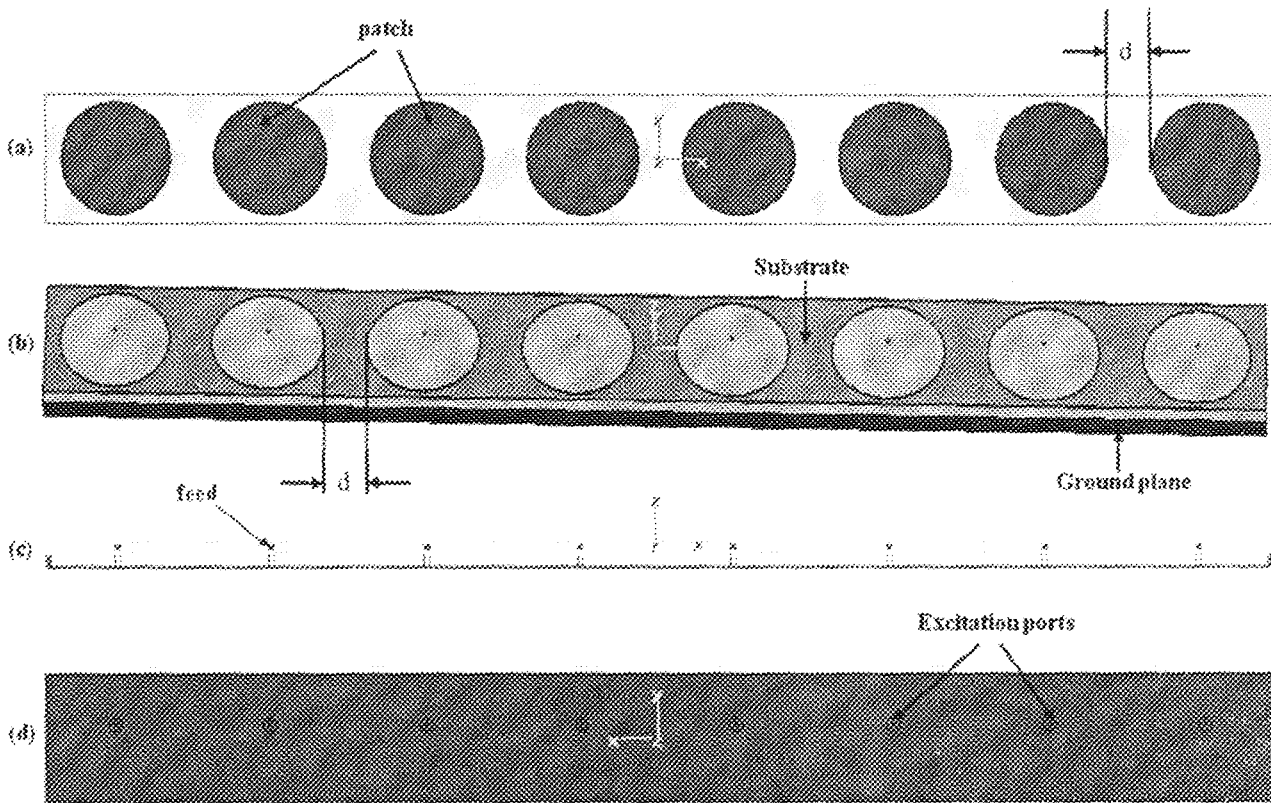


Fig 3.3: The 8x1 patch antenna array feed for 6 GHz with inter-element spacing d

(a) Top view, (b) Perspective view, (c) Wireframe view, (d) Bottom view (using CST MWS)

3.3.1 Assumptions for the patch antenna array design

The following are the assumptions made for the purpose of this design:

- i. The array configuration is perfectly linear
- ii. The inter-element distance for the patch antenna array elements is equal.
- iii. The array elements have uniform signal excitation amplitude.
- iv. The array elements have uniform phase.
- v. All the elements in the array have identical patterns.
- vi. The array configuration is symmetric about the mid-point.

The first step in this approach is to calculate the uniform array inter-element distance that will give us our required beamwidth of 140° with uniform normalized array element excitation amplitude. Then the Genetic Algorithm (GA) optimization technique will be utilized to vary the excitation of each array element while keeping the inter-element distance constant to achieve minimum sidelobes and maximum energy on the main lobe for the patch antenna array.

3.3.2 Modeling the inter-element distance

The first null beamwidth (FNBW) is selected to minimize illumination loss. Beamwidth for uniform amplitude broadside arrays can be calculated by the following relation (Balanis, 2005),

$$\theta_n = 2 \left[\frac{\pi}{2} - \cos^{-1} \left(\frac{\lambda}{Nd} \right) \right] \quad (3.11)$$

where θ_n is the first null beam width, λ is the wavelength, N is the number of array elements and d is the uniform inter-element distance in cm. Leaning on the earlier indicated assumption of a symmetry about the mid-point for the broadside configuration, we can say that;

$$\cos \left[\frac{\pi}{2} - \frac{\theta_n}{2} \right] = \cos \left[\cos^{-1} \left(\frac{\lambda}{Nd} \right) \right] \quad (3.12)$$

From trigonometric relations, this becomes

$$\sin \frac{\theta_n}{2} = \frac{\lambda}{Nd} \quad (3.13)$$

Therefore, inter-element distance d is given by

$$d = \frac{\lambda}{N \sin \left(\frac{\theta_n}{2} \right)} \quad (3.14)$$

For the C-band patch antenna array, the resonant frequency of 6 GHz corresponds to a wavelength λ given by

$$\lambda = \frac{v}{f} \quad (3.15)$$

Here, v = speed of electromagnetic radiation = 3×10^8 m/s

Thus, substituting values, the wavelength is computed as

$$\lambda = \frac{3 \times 10^8}{6 \times 10^9} = 0.05 \text{ m} = 5.0 \text{ cm} \quad (3.16)$$

Substituting values, gives the inter-element distance as

$$d = \frac{5.0}{8 \sin\left(\frac{140^\circ}{2}\right)} \cong 0.67 \text{ cm} \quad (3.17)$$

Therefore, the patch antenna array inter-element distance is $0.67 \text{ cm} = 0.133 \lambda$

The radiation pattern for this configuration is depicted in figure 3.4.

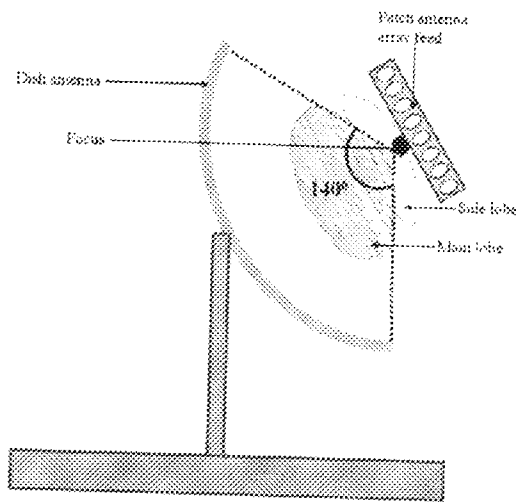


Figure 3.4: Aperture Illumination = First Null Beam Width (FNBW) = 140°

3.4 Genetic Algorithm optimization of the patch antenna array

For the patch antenna array, Genetic Algorithm (GA) is used to tailor the design in order to achieve a radiation pattern with maximum sidelobe level reduction at 140° first null beamwidth (FNBW). In this case, the design problem consists of finding amplitude-tapered weights that give a radiation pattern with minimum sidelobe level. The linear 8×1 uniformly spaced broadside

patch antenna array, with its elements symmetrically situated and with symmetrical amplitude excitation around the centre is adapted.

3.4.1 Amplitude tapering using Genetic Algorithm

The optimization method was based on real-coded genetic algorithm (GA) with elitist strategy for the antenna excitation amplitude tapering. Real-coded GA uses floating-point number representation for the real variables and thus is free from binary encoding and decoding (Michalewicz, 1999). In floating-point representation, each chromosome or individual weight vector represents excitation amplitude vector of each patch antenna element. A flow chart diagram of real-coded GA employed in this work is shown in Figure 3.5.

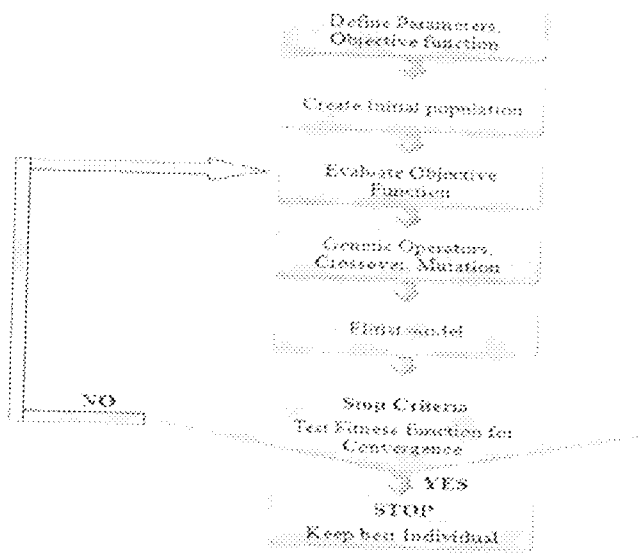


Fig 3.5: Flow chart of the Genetic Algorithm Process

3.4.2 Step 1: Define Parameters, Fitness function

A linear array of 8 patch antennas was considered, in which the antennas were assumed uncoupled (coupling causes variation in the element impedance, reflection coefficients, and overall antenna pattern in a finite element array), symmetrically situated, conjugated

symmetrically excited around the center, and equally spaced with inter-element distance 0.14 wavelength apart along the x-axis. The array factor (AF) for normalized, linear, uniformly spaced, non-uniform amplitude, broadside 8-element arrays is given by the following equation (Balanis, 2005).

$$AF = \sum_{n=1}^4 a_n \cos \left[\frac{(2n-1)}{2} \psi \right] \quad (3.18)$$

where $\psi = kd \cos \theta + \beta$

a_n = amplitude excitation of the n th element.

β = progressive phase shift between individual elements.

$k = 2\pi/\lambda$ is the wave number.

d = inter-element spacing

θ = angle between the axis of the array (x -axis) and the radial vector from the origin to the observation point.

The GA synthesis is therefore reduced to the search of the excitation amplitude defined by the vector $w = (a_1 \ a_2 \ \dots \ a_n)$ which is the weight vector constituting the amplitude-tapered weights of the respective elements. Here, we are interested in designing an antenna array with minimum sidelobe levels for a specific first null beamwidth (FNBW) which in this case is 140° . Considering the case of broadside array radiation with the main lobe maximum radiation at 90° , the fitness function (FF) employed is the total average sidelobe level (equation (3.19)). By this we refer to the addition of the average side lobe level between $-\pi/2$ and the first null before the boresight (θ_{nu1}) to the average sidelobe level between the first null after the boresight (θ_{nu2}) and $3\pi/2$.

$$FF = \frac{1}{\theta_{nu1} + \frac{\pi}{2}} \int_{-\frac{\pi}{2}}^{\theta_{nu1}} |AF\theta| d\theta + \frac{1}{\frac{3\pi}{2} - \theta_{nu2}} \int_{\theta_{nu2}}^{\frac{3\pi}{2}} |AF\theta| d\theta \quad (3.19)$$

$$\theta_{nu1} = 20^\circ$$

$$\theta_{nu2} = 160^\circ$$

$$\theta_{nu2} - \theta_{nu1} = 140^\circ (\text{FNBW})$$

Because of the symmetry, the two expressions on the right side of equation (3.19) are the same so only one is enough to evaluate the fitness function.

3.4.3 Step 2: Create Initial population

Each chromosome was used to represent a patch antenna element. Each gene of an individual chromosome was used to represent the excitation amplitude of a single patch antenna array element. For a linear array of '8' antenna elements an initial population of **P** individual chromosomes (amplitude vectors), each consisting of **N** genes, was randomly generated. The normalized values of the excitation amplitude are being considered here. Therefore, the generated population has a gene value constraint range between 0 and 1.

$$\begin{aligned} \text{Initial population}(P) &= \begin{bmatrix} w_1 \\ \vdots \\ w_P \end{bmatrix} \\ &= \begin{bmatrix} \text{gene}_{1,1} & \dots & \text{gene}_{1,8} \\ \vdots & \ddots & \vdots \\ \text{gene}_{10,1} & \dots & \text{gene}_{10,8} \end{bmatrix} \end{aligned} \quad (3.20)$$

where the amplitude vector (chromosome) $w = [\text{gene}_1 \dots \text{gene}_8] = [a_1 \dots a_8]$

GA starts with an arbitrary solution created by a random number generator. In this particular problem, it is equivalent to starting with randomly generated values for the array parameters (amplitude excitations), which will be determined. Solutions are represented with vectors of the parameter values as the initial population of the GA.

Number of parameters = 8 (number of amplitude excitations)

$$=[a_1 \quad \dots \quad a_8]$$

Initial population \mathbf{P} chosen, $\mathbf{P} = 10$ chromosomes

The initial population randomly generated is a matrix of dimension 10×8 shown in equation (3.18), with each row corresponding to a chromosome and each column in a chromosome corresponding to the excitation amplitude of a single antenna (patch) element.

$$\mathbf{P} = \begin{bmatrix} 0.8147 & 0.1576 & 0.6557 & 0.7060 & 0.4387 & 0.2760 & 0.7513 & 0.8407 \\ 0.9058 & 0.9706 & 0.0357 & 0.0318 & 0.3816 & 0.6797 & 0.2551 & 0.2543 \\ 0.1270 & 0.9572 & 0.8491 & 0.2769 & 0.7655 & 0.6551 & 0.5060 & 0.8143 \\ 0.9134 & 0.4854 & 0.9340 & 0.0462 & 0.7952 & 0.1626 & 0.6991 & 0.2435 \\ 0.6324 & 0.8003 & 0.6787 & 0.0971 & 0.1869 & 0.1190 & 0.8909 & 0.9293 \\ 0.0975 & 0.1419 & 0.7577 & 0.8235 & 0.4898 & 0.4984 & 0.9593 & 0.3500 \\ 0.2785 & 0.4218 & 0.7431 & 0.6948 & 0.4456 & 0.9597 & 0.5472 & 0.1966 \\ 0.5469 & 0.9157 & 0.3922 & 0.3171 & 0.6463 & 0.3404 & 0.1386 & 0.2511 \\ 0.9575 & 0.7922 & 0.6555 & 0.9502 & 0.7094 & 0.5853 & 0.1493 & 0.6160 \\ 0.9649 & 0.9595 & 0.1712 & 0.0344 & 0.7547 & 0.2238 & 0.2575 & 0.4733 \end{bmatrix} \quad (3.21)$$

3.4.4 Step 3: Evaluate Objective function Fitness function

Objective function is used to evaluate individual chromosome fitness. The input to the objective function is a chromosome which is the normalized excitation amplitude weight vector of the array elements. The output of the objective function is known as the cost which qualifies the fitness of each individual. The objective function, whenever called upon, evaluates the array factor radiation pattern with the sidelobe level value of the antenna array for each individual

chromosome. The evaluation continues for the entire population with each sidelobe level value assigned a cost to qualify its fitness. Low cost signifies high fitness and vice versa.

The chromosomes from step 2 are passed to the objective function for evaluation. The objective function evaluates each of the 10 chromosomes and then outputs their respective costs (Side lobe level value) as shown in equation (3.19). The amplitude vector that provides the lowest side lobe level is that of the ninth chromosome with **cost = -15.6394**.

$$[\text{Chrom} \quad \text{Cost}] = \begin{bmatrix} 1 & -9.3203 \\ 2 & -7.1238 \\ 3 & -11.3353 \\ 4 & -8.3048 \\ 5 & -7.6505 \\ 6 & -6.7115 \\ 7 & -8.8157 \\ 8 & -11.4422 \\ 9 & -15.6394 \\ 10 & -8.9905 \end{bmatrix} \quad (3.22)$$

3.4.5 Step 4: Selection

The highest fit individuals (healthiest members of population) having the least cost are then selected using ranking method and placed in the mating pool. Numbers of individuals in the mating pool are same as P in order to accommodate more copies of superior individuals in the new population. The costs were sorted in order to determine the relative fitness of the chromosomes. Five, out of the ten (representing a fitness factor of 0.5) highest fit chromosomes are selected and placed in the mating pool to become parents of the next generation, whilst the rest are discarded. The fitness factor of 0.5 was chosen to facilitate generation quality retention.

Sorting the cost gives:

$$[\text{Chrom Cost}] = \begin{bmatrix} 9 & -15.6394 \\ 8 & -11.4422 \\ 3 & -11.3353 \\ 1 & -9.3203 \\ 10 & -8.9905 \\ 7 & -8.8157 \\ 4 & -8.3048 \\ 5 & -7.6505 \\ 2 & -7.1238 \\ 6 & -6.7115 \end{bmatrix} \quad (3.23)$$

The chromosomes to be placed in the mating pool as parents of the next generation are 9,8,3,1, and 10.

$$[\text{Chrom Cost}] = \begin{bmatrix} 0.9575 & 0.7922 & 0.6555 & 0.9502 & 0.7094 & 0.5853 & 0.1493 & 0.6160 & -15.6394 \\ 0.5469 & 0.9157 & 0.3922 & 0.3171 & 0.6463 & 0.3404 & 0.1386 & 0.2511 & -11.4422 \\ 0.1270 & 0.9572 & 0.8491 & 0.2769 & 0.7655 & 0.6551 & 0.5060 & 0.8143 & -11.3353 \\ 0.8147 & 0.1576 & 0.6557 & 0.7060 & 0.4387 & 0.2760 & 0.7513 & 0.8407 & -9.3203 \\ 0.9649 & 0.9595 & 0.1712 & 0.0344 & 0.7547 & 0.2238 & 0.2575 & 0.4733 & -8.9905 \end{bmatrix} \quad (3.24)$$

3.4.6 Step 5: Crossover and Mutation

The parents were allowed to mate in the mating pool, followed by mutation using heuristic crossover and uniform mutation respectively. In the crossover process, two parents mate each other to produce two children. Subsequent mutations of the parents add diversity to the population and explore new areas of parameter search space. A mutation rate of 1.0% was used to achieve best fit generation without premature convergence together with heuristic crossover to produce offspring that are now parents of the next generation as shown in equation (3.23).

$$P = \begin{bmatrix} 0.9575 & 0.7922 & 0.6555 & 0.9502 & 0.7094 & 0.5853 & 0.1493 & 0.6160 \\ 0.5469 & 0.9157 & 0.3922 & 0.3171 & 0.6463 & 0.3404 & 0.1386 & 0.2511 \\ 0.1270 & 0.9572 & 0.8491 & 0.2769 & 0.7655 & 0.6551 & 0.5060 & 0.8143 \\ 0.8147 & 0.1576 & 0.6557 & 0.7060 & 0.4387 & 0.2760 & 0.7513 & 0.8407 \\ 0.9649 & 0.9595 & 0.1712 & 0.0344 & 0.7547 & 0.2238 & 0.2575 & 0.4733 \\ 0.1270 & 0.9572 & 0.8491 & 0.2769 & 0.7596 & 0.2238 & 0.2575 & 0.4733 \\ 0.9649 & 0.9595 & 0.1712 & 0.0344 & 0.7606 & 0.6551 & 0.5060 & 0.8143 \\ 0.1270 & 0.9572 & 0.8491 & 0.2769 & 0.7655 & 0.6551 & 0.3187 & 0.4733 \\ 0.1641 & 0.1576 & 0.6557 & 0.7060 & 0.4387 & 0.2760 & 0.7513 & 0.8407 \\ 0.7776 & 0.9572 & 0.8491 & 0.2769 & 0.7655 & 0.6551 & 0.5060 & 0.8143 \end{bmatrix} \quad (3.24)$$

3.4.7 Step 6: Elitist model

The postprocessor is the elitist model. The worst individuals in the newly generated populations are replaced by the best individuals in the old population. This is adopted to ensure the algorithm's convergence. This step has been introduced to prevent losing the best found individual chromosomes by chance because of crossover and mutation. It will always preserve the best chromosome from one generation to the next. Therefore, the costs of the population in the current generation (gen+1) from step 5 were compared to those of the preceding population in generation (gen) after sorting and the result is given in equation (3.23).

$$[(\text{gen} + 1) \quad (\text{gen})] = \begin{bmatrix} -15.6394 & -15.6394 \\ -14.8494 & -11.4422 \\ -11.4422 & -11.3353 \\ -11.0342 & -9.3203 \\ -10.0137 & -8.9905 \\ -9.0964 & -8.8157 \\ -8.4383 & -8.3048 \\ -8.0020 & -7.6505 \\ -7.7495 & -7.1238 \\ -7.6047 & -6.7115 \end{bmatrix} \quad (3.26)$$

On comparison, we observe that the current generation (gen +1) is better fit than the preceding generation (gen) and therefore elitism will not be applicable in this case.

3.4.8 Step 7: Stop Criteria and final result

The stopping criterion is 100 generations. So steps 3 to 6 were repeated until the stopping criterion was reached.

[Chrom Cost]

$$= \begin{bmatrix} 0.99038 & 0.76528 & 0.45144 & 0.1718 & 0.1718 & 0.45144 & 0.76528 & 0.99038 & - & 35.071 \\ 0.99038 & 0.76528 & 0.45144 & 0.1718 & 0.1718 & 0.45144 & 0.76528 & 0.99038 & - & 35.071 \\ 0.99038 & 0.76528 & 0.45144 & 0.1718 & 0.1718 & 0.45144 & 0.76528 & 0.99038 & - & 35.071 \\ 0.99038 & 0.76528 & 0.45144 & 0.1718 & 0.1718 & 0.45144 & 0.76528 & 0.99038 & - & 35.071 \\ 0.99038 & 0.76528 & 0.45144 & 0.1718 & 0.1718 & 0.45144 & 0.76528 & 0.99038 & - & 35.071 \\ 0.99038 & 0.76528 & 0.45144 & 0.1718 & 0.1718 & 0.45144 & 0.76528 & 0.99038 & - & 35.071 \\ 0.99038 & 0.76528 & 0.45144 & 0.1718 & 0.1718 & 0.45144 & 0.76528 & 0.99038 & - & 35.071 \\ 0.99038 & 0.76528 & 0.45144 & 0.1718 & 0.1718 & 0.45144 & 0.76528 & 0.99038 & - & 35.071 \\ 0.99038 & 0.76528 & 0.45144 & 0.1718 & 0.1718 & 0.45144 & 0.76528 & 0.99038 & - & 35.071 \\ 0.99038 & 0.76528 & 0.45144 & 0.1718 & 0.1718 & 0.45144 & 0.76528 & 0.99038 & - & 35.071 \end{bmatrix} \quad (3.27)$$

From the result, it is evident that after passing through the generations all of the final solutions have converged to a global optimum. This is observed to occur after 50 generations (see figure 3.6). This means that the combination of all the individual chromosomes representing the antenna array excitation amplitude tapered weights can provide a radiation pattern with the maximum possible side lobe level reduction at this point.

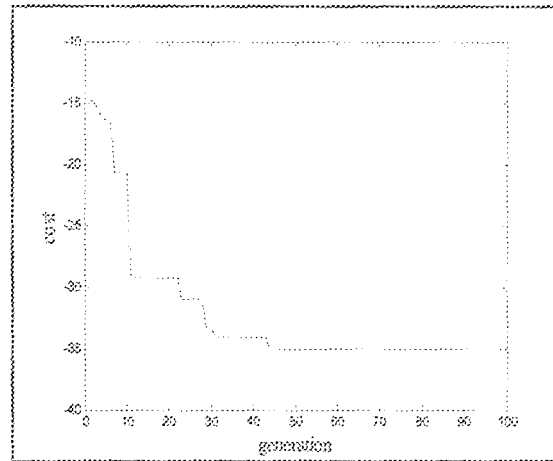


Fig 3.6: Performance graph of the optimization process

This means that the normalized excitation amplitudes for the 8x1 patch antenna array elements of the feed that will result in the lowest sidelobe level for the radiation pattern at 140° first null beam width (FNBW) are shown in Table 3.1.

Table 3.1: GA optimized normalized excitation amplitudes for the antenna array elements

Array element Excitation port	1	2	3	4	5	6	7	8
Normalized excitation amplitude	0.9904	0.7653	0.4514	0.1718	0.1718	0.4514	0.7653	0.9904

3.5 Varying inter-element distance

The second approach to the design of the patch antenna array feed is to vary the beamwidth between the first nulls (FNBW) while keeping the normalized signal excitation amplitudes and phases of the array elements uniform and constant. This can be achieved by varying the inter-element distance. Conventional feeds have a wide main lobe that maximizes the illumination efficiency. The best efficiency occurs when the illumination energy is about 10 dB down at the edge of the dish (Wade, 2003).

Backed with this fact, the patch antenna array feed design will try to achieve a FNBW that exceeds 140° . This will ensure that the 10 dB point on the main lobe falls within the aperture of the dish antenna. Going back to equation (3.11), it can be seen that the equation is valid for the

values $0 \leq \left| \frac{\lambda}{Nd} \right| \leq 1$

And when, inter-element distance $d = \frac{\lambda}{N}$

$$\frac{\lambda}{Nd} = 1, \cos^{-1}\left(\frac{\lambda}{Nd}\right) = 0 \tag{3.28}$$

Thus, First Null beamwidth (FNBW), $\theta_n = 2 \left[\frac{\pi}{2} - \cos^{-1}(1) \right]$ (3.29)

That is, $\theta_n = \pi$ (3.30)

Therefore, to achieve a first null beamwidth (FNBW) of 180° , for the 4×1 patch antenna array, where wavelength λ is 5cm and N is 4, the inter-element distance is

$$d = \frac{5}{8} = 0.63\text{cm} = 0.125 \lambda \quad (3.31)$$

The radiation pattern for this configuration is depicted in figure (3.7).

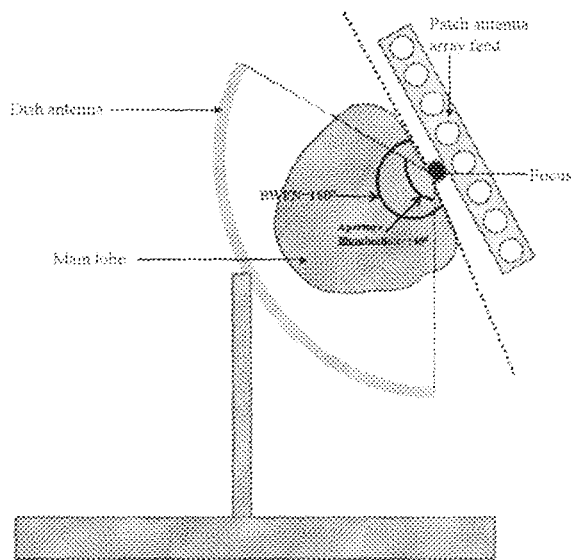


Fig 3.7: Patch antenna array feed with inter-element distance, 1.25cm
Aperture Illumination = 140° , First Null Beam Width (FNBW) = 180°

CHAPTER FOUR

4.0 RESULTS

In the preceding chapter, two approaches to the design of a patch antenna array feed for C-Band dish antenna were considered. The dish antenna selected is with F/D of 3.6 which corresponds to an aperture illumination of 140° . To maintain a simple geometry and configuration for the patch antenna array, an 8×1 linear array configuration was chosen with a broadside radiation pattern. The first approach was to eliminate illumination loss and maximize the gain. Keeping the calculated inter-element distance constant, the excitation amplitudes of the array elements were varied using Genetic Algorithm (GA) to achieve minimum sidelobe levels.

The second approach was to widen the main beamwidth and concentrate the stronger part of the beam on the aperture. The main beamwidth was varied while keeping the normalized signal excitation amplitudes and phases of the array elements uniform and constant. The array designs resulting from these two approaches will be simulated and their performances will be analyzed in this chapter.

4.1 The patch antenna array feed (FNBW = Aperture Illumination = 140°)

To accomplish the thesis objective, the software utilized was Personal Computer Aided Antenna Design (PCAAD 5.0). This software, based on the method of moments (MOM) was used to simulate the array feed and analyze the RF characteristics. PCAAD 5.0 is a specialized tool for fast and accurate three dimensional electromagnetic simulations of high frequency problems. The GA optimized patch antenna array feed (parameters in table 3.1) was simulated using PCAAD

5.0. The PC screen display of the PCAAD 5.0 is shown in appendixes A, B and C. The simulated far field radiation pattern plots are shown in the figures 4.1-4.3.

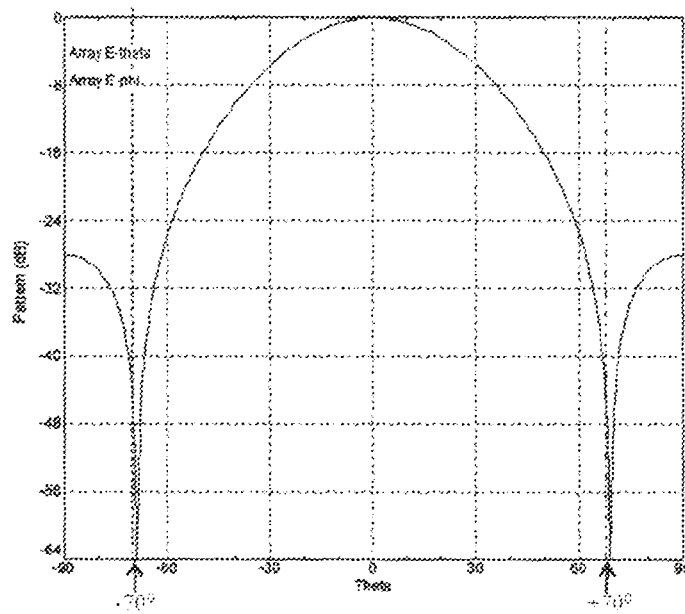


Fig. 4.1: Rectangular planar radiation pattern plot for 8X1 patch antenna array feed, $d = 0.67\text{cm}$ (using PCAAD 5.0)

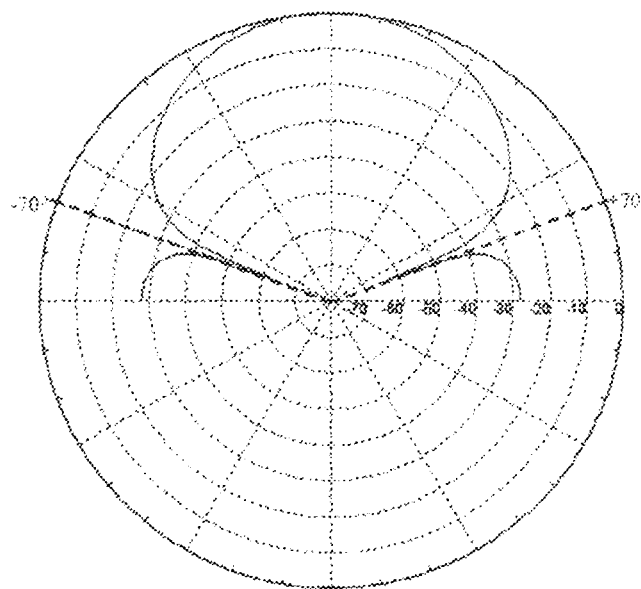


Fig. 4.2: Polar radiation pattern plot for 8X1 patch antenna array feed, $d = 0.67\text{cm}$ (using PCAAD 5.0)

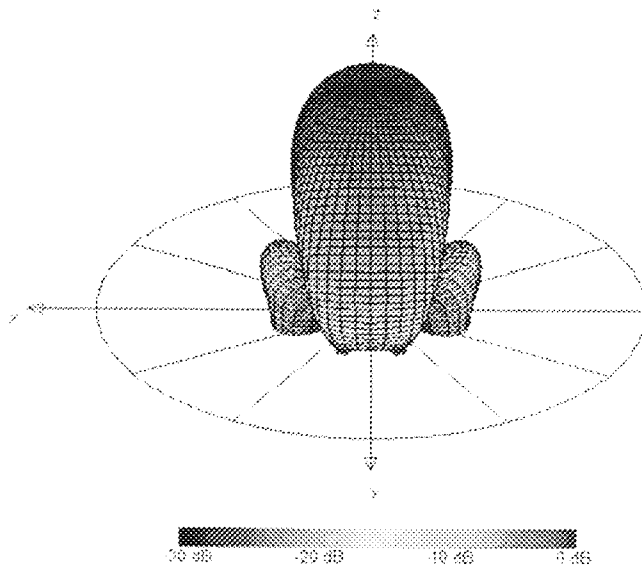


Fig. 4.3: 3-D Radiation pattern plot for 8X1 patch antenna array feed, $d = 0.67\text{cm}$
(using PCAAD 5.0)

From the radiation pattern plots in figures 4.1-4.3, we obtain a 3 dB beamwidth of 44.2°

4.2 The patch antenna array feed (FNBW = 180°)

The 8X1 patch antenna array feed configuration with FNBW = 180° corresponding to an inter-element distance of 0.625cm was simulated. The simulated far field radiation pattern plots are shown in the figures 4.4-4.6.

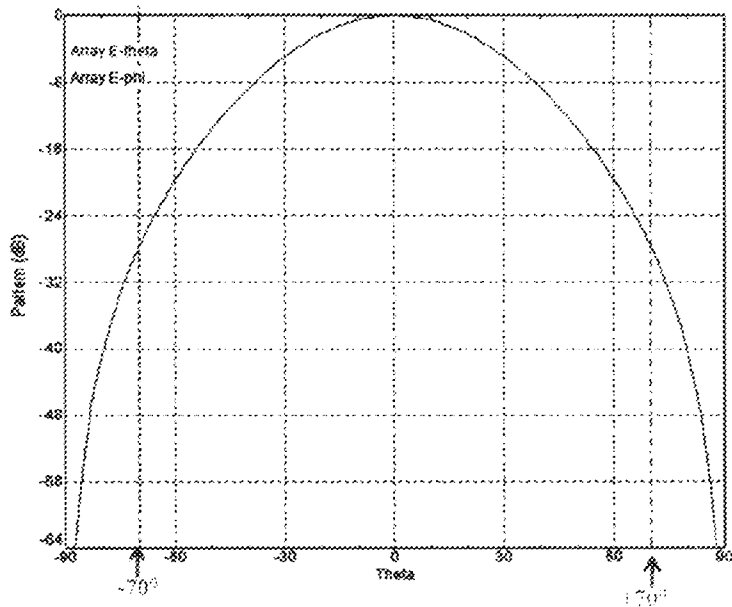


Fig. 4.4: Rectangular planar radiation pattern plot for 8X1 patch antenna array feed, $d = 0.625\text{cm}$
 (using PCAAD 5.0)

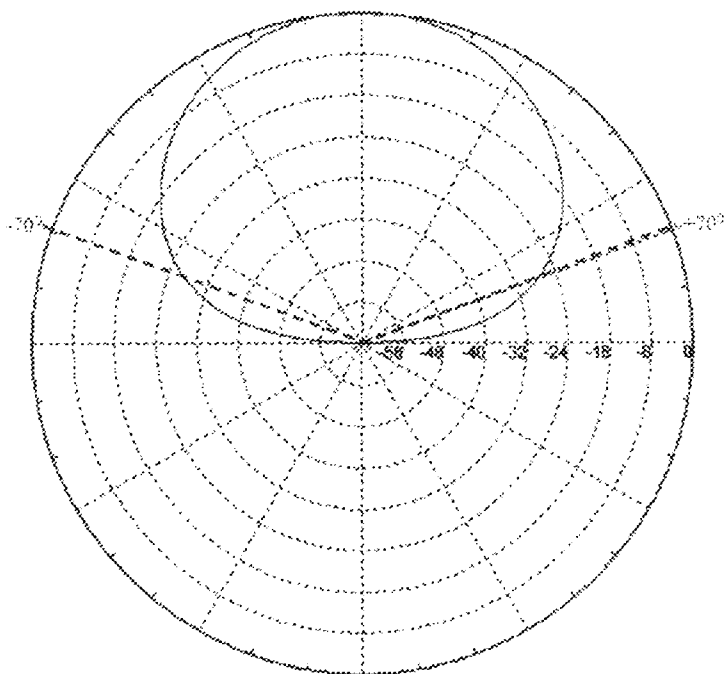


Fig. 4.5: Polar radiation pattern plot for 8X1 patch antenna array feed, $d = 0.625\text{cm}$
 (using PCAAD 5.0)

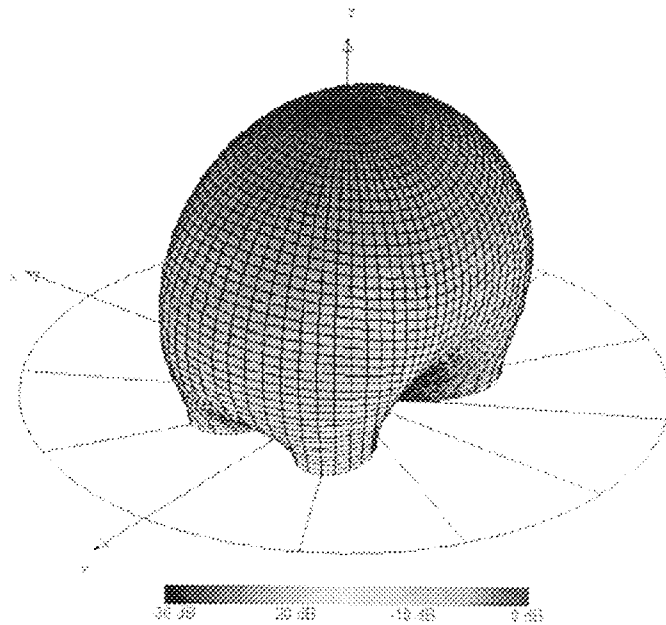


Fig. 4.6: 3-D Radiation pattern plot for 8X1 patch antenna array feed, $d = 0.625\text{cm}$
(using PCAAD 5.0)

From the radiation pattern plots in figures 4.4-4.6, we observe that the feed pattern radiated over the effective aperture of the dish is continuous with an illumination taper of 27.8 dB. The 3 dB beamwidth has widened to 46.87° implying that more energy is concentrated on the effective aperture of the dish. The illumination taper for this continuous pattern is not so efficient when compared with the 10dB required (Wade, 2003).

Further simulations were carried out on inter-element distances, $d = 0.5\text{cm}$ and $d = 1.35\text{cm}$ (corresponding to inter-element distance, $d > \lambda/4$) to find out the effect on the radiation pattern presented by the 8X1 patch antenna array feed for the C-Band dish. The simulated far field radiation pattern plots are shown in the figures 4.7-4.9.

4.3 The patch antenna array feed (Inter-element distance = 0.5cm)

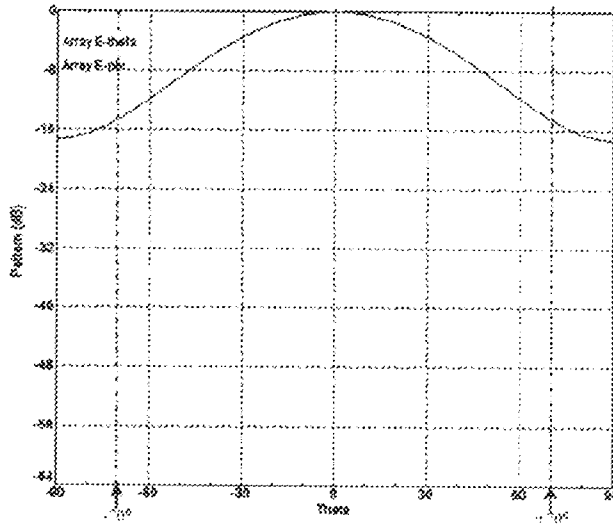


Fig. 4.7: Rectangular planar radiation pattern plot for 8X1 patch antenna array feed, $d = 0.5\text{cm}$ (using PCAAD 5.0)

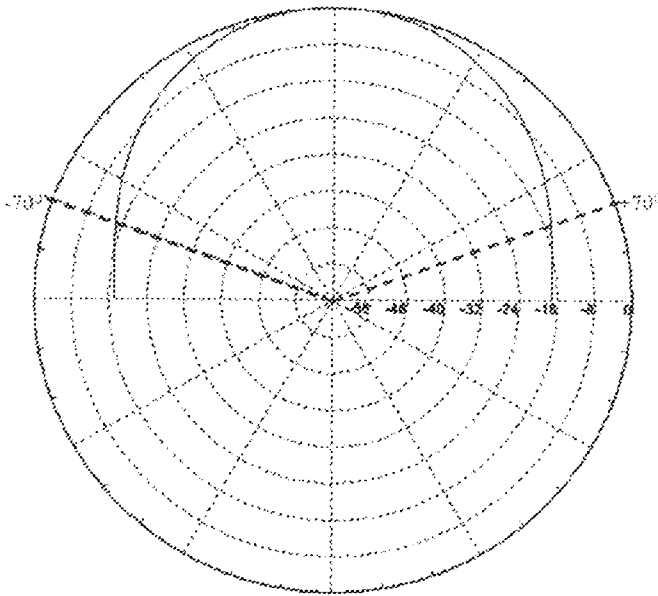


Fig. 4.8: Polar radiation pattern plot for 8X1 patch antenna array feed, $d = 0.5\text{cm}$ (using PCAAD 5.0)

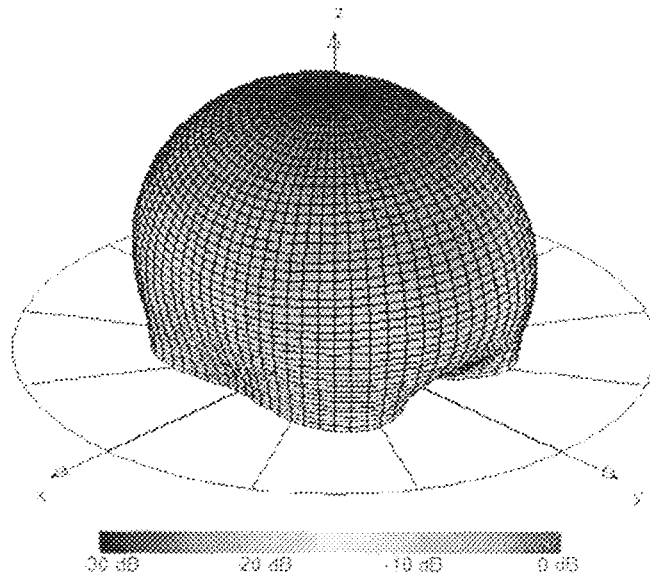


Fig. 4.9: 3-D Radiation pattern plot for 8X1 patch antenna array feed, $d = 0.5\text{cm}$
(using PCAAAD 5.0)

From the radiation pattern plots for the 8X1 patch antenna array feed for inter-element distance, $d = 0.5\text{cm}$ shown in figures 4.7-4.9, it is observed that the feed pattern radiated over the effective aperture of the dish is continuous with an improved illumination taper of 14.5dB. The 3 dB beamwidth has widened to 56.06° implying that even more energy is concentrated on the effective aperture of the dish. The illumination taper is comparable to the 10dB required (Wade, 2003).

4.4 The patch antenna array feed (Inter-element distance $> \lambda/4$)

The simulated radiation pattern plots for the patch antenna array feed for inter-element distance, $d = 1.35\text{cm}$ are presented in figures 4.10-4.12. For this configuration, where the inter-element distance is greater than one quarter wavelength, it is observed that the feed pattern radiated over the aperture of the dish includes four nulls at -30° , $+30^\circ$, -70° and $+70^\circ$ accompanied with

substantial side lobes. The presence of the nulls and sidelobes has a tendency of reducing the overall aperture efficiency of the dish for this configuration.

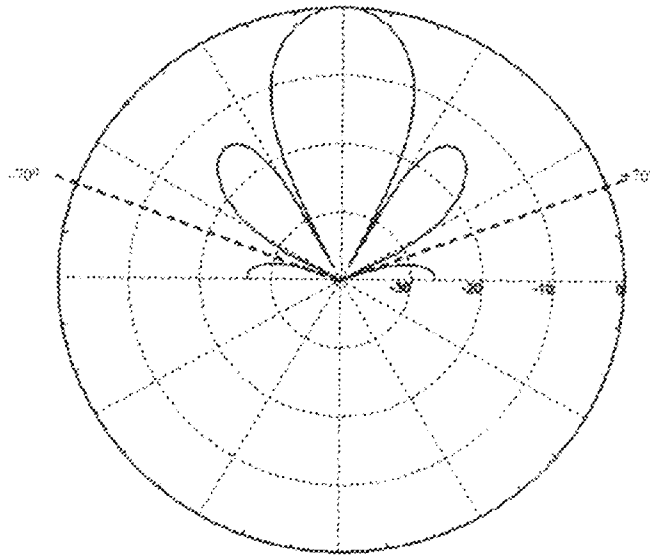


Fig. 4.10: Polar radiation pattern plot for 8X1 patch antenna array feed, $d = 1.35\text{cm}$
(using PCAAD 5.0)

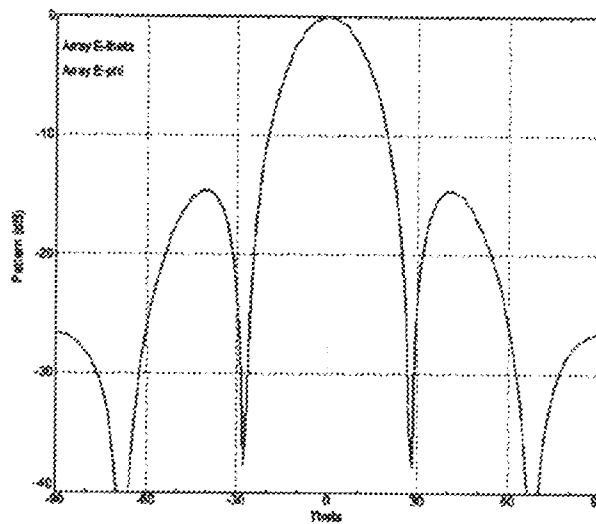


Fig. 4.11: Rectangular planar radiation pattern plot for 8X1 patch antenna array feed, $d = 1.35\text{cm}$
(using PCAAD 5.0)

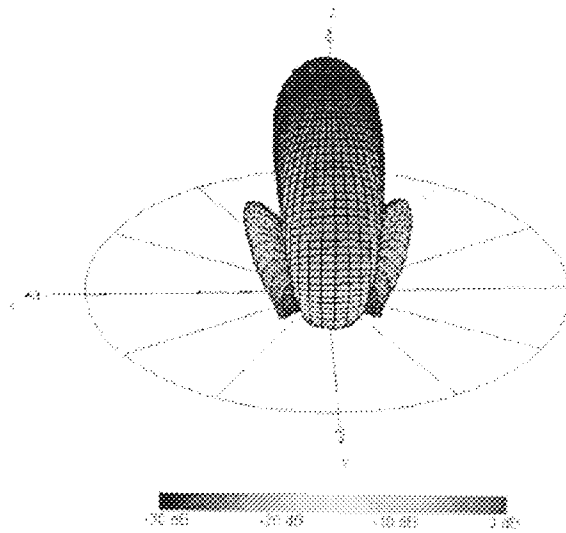


Fig. 4.12: 3-D Radiation pattern plot for 8X1 patch antenna array feed, $d = 1.35\text{cm}$
(using PCAAD 5.0)

4.5 Efficiency Computation

The illumination efficiency of the C-Band 8X1 patch antenna array feed for each inter-element distance is calculated by integrating the feed pattern radiated over the area of the reflector and dividing it by the total integrated feed pattern (Wade, 2003). This is done in this case by integrating the radiation pattern over the effective aperture of the dish antenna (20° to 160°) and dividing it by the total integrated pattern (0° to 360°) with the assumption of uniform array element excitation amplitude and phase. Also, the other efficiency components mentioned in Section 2.1 are not considered. This modifies the equation (3.18) to become

$$AF(\theta) = \sum_{n=1}^4 a_n \cos \left[\frac{(2n-1)}{2} kd \cos \theta \right] \quad (4.1)$$

Thus,

$$Efficiency = \frac{\int_{20^\circ}^{160^\circ} |AF| d\theta}{\int_{0^\circ}^{360^\circ} |AF| d\theta} \quad (4.2)$$

This analysis was carried out using MATLAB (see source code in appendix E) with a uniform radiated power of 0 dB on each array element of the 8X1 patch antenna array feed. The progressive phase shift, β between individual elements was also taken to be 0. The result of this analysis is presented in Figures 4.13 and 4.14.

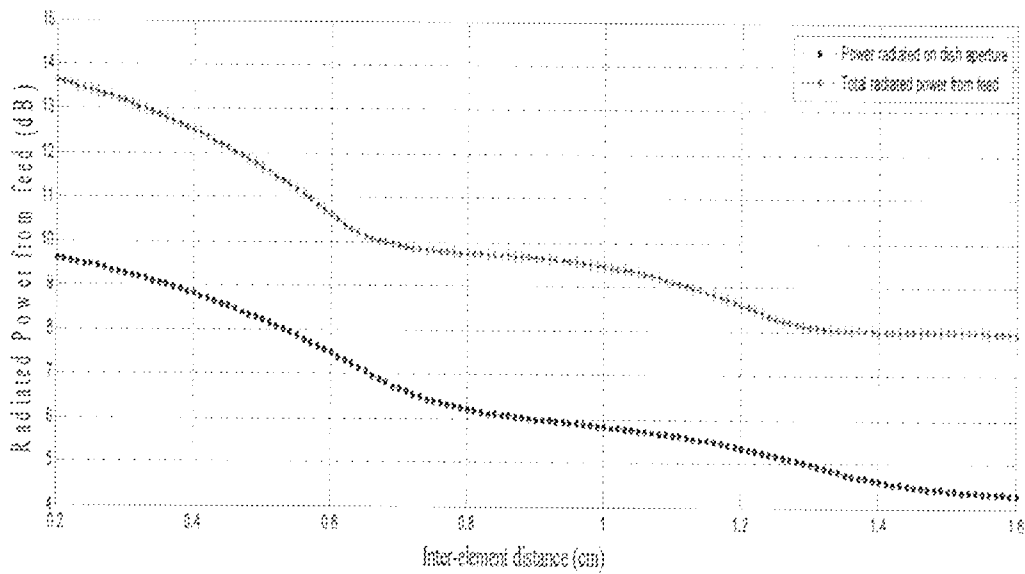


Fig. 4.13: Inter-element distance vs Radiated Power for the C-Band patch antenna array feed

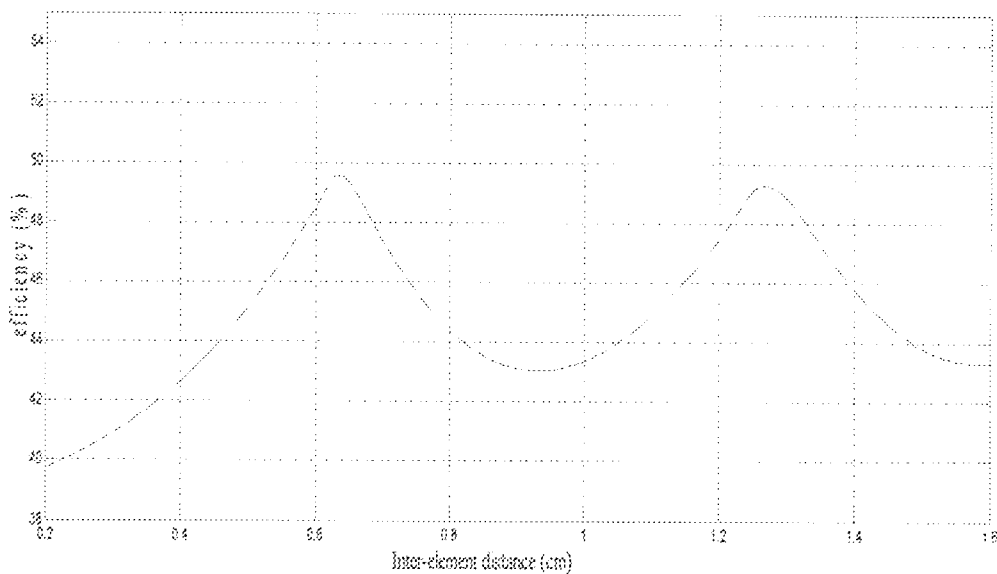


Fig. 4.14: Inter-element distance vs illumination Efficiency for the C-Band patch antenna array feed

CHAPTER FIVE

5.0 DISCUSSION, CONCLUSION AND RECOMMENDATION

5.1 Introduction

Two approaches to the design of the 8X1 patch antenna array feed for C-Band dish ($F/D=0.36$) have been considered. The designs were simulated and the results of the simulations were analyzed. From the graphs and simulations, it is observed that for the patch antenna array feed, the total radiated power decreases with increasing uniform inter-element distances for a uniform array element amplitude excitation. Similarly, the total radiation over the effective aperture of the dish antenna decreases with increasing inter-element spacing for this configuration. This means that ideally, the elements should be kept closer to achieve a higher gain from the feed. This however has its limitations because the aperture efficiency was also observed to decrease progressively as the inter-element distance is moved away (either positively or negatively) from 0.63cm which is about $\lambda/8$.

Therefore, it can be inferred that the ideal inter-element spacing for the 8X1 patch antenna array feed for C-Band dish ($F/D=0.36$) is about 0.63cm ($\approx\lambda/8$) in order to achieve good aperture efficiency and gain for the feed. At this spacing, the simulated efficiency while keeping all the other efficiency components constant is about 49.6%. This is very competitive when compared to that achieved with conventional feeds for the same F/D ratio of 0.36 which is between 50-75% (Wade, 2003). Also at this spacing, the total weight of the feed is 91.3g and total array length is approximately 18.5cm which satisfies the condition of reduced weight and dimensions required for on-board satellite applications where mass and size limitations are extremely strict.

Table 5.1: Weight and Dimensions Comparison for the designed patch antenna array with conventional Radially Corrugated Horn feed for C-Band dish antenna

C-BAND DISH FEED TYPE	WEIGHT(g)	LENGTH(cm)	HEIGHT(cm)
Patch Antenna Array	91.3	18.5	0.367
Radially Corrugated Horn (NIGCOMSAT-1)	9300	25	30

5.2 Recommendations

The patch antenna array feed is recommended for C-Band and higher band dishes on board a satellite mainly because of its compactness and light weight. Future works should focus more on the underlisted areas for improvement on the efficiency.

5.2.1 Aperture illumination

The effect of varying the aperture illumination (F/D ratio) for the dish antenna on the performance of the feed with respect to gain and efficiency should be investigated for this configuration. This will help in determining the most suitable F/D ratio.

5.2.2 Patch antenna element configuration

Other patch antenna array element configurations such as square, triangular, elliptical, circular ring, and so on should be investigated to determine how the element configuration affects the aperture efficiency of the selected dish aperture illumination.

5.2.3 Array Configuration

Other patch antenna array feed configurations like planar and cylindrical should be investigated including configurations with non-uniform inter-element distances, phases and amplitude excitations. This will enable the determination of the effect of the different configurations on the total radiated power from the feed, gain, beamwidth and the aperture efficiency. The effect of the number of array elements on the performance should also be analyzed. All these will serve as a tool for antenna designers.

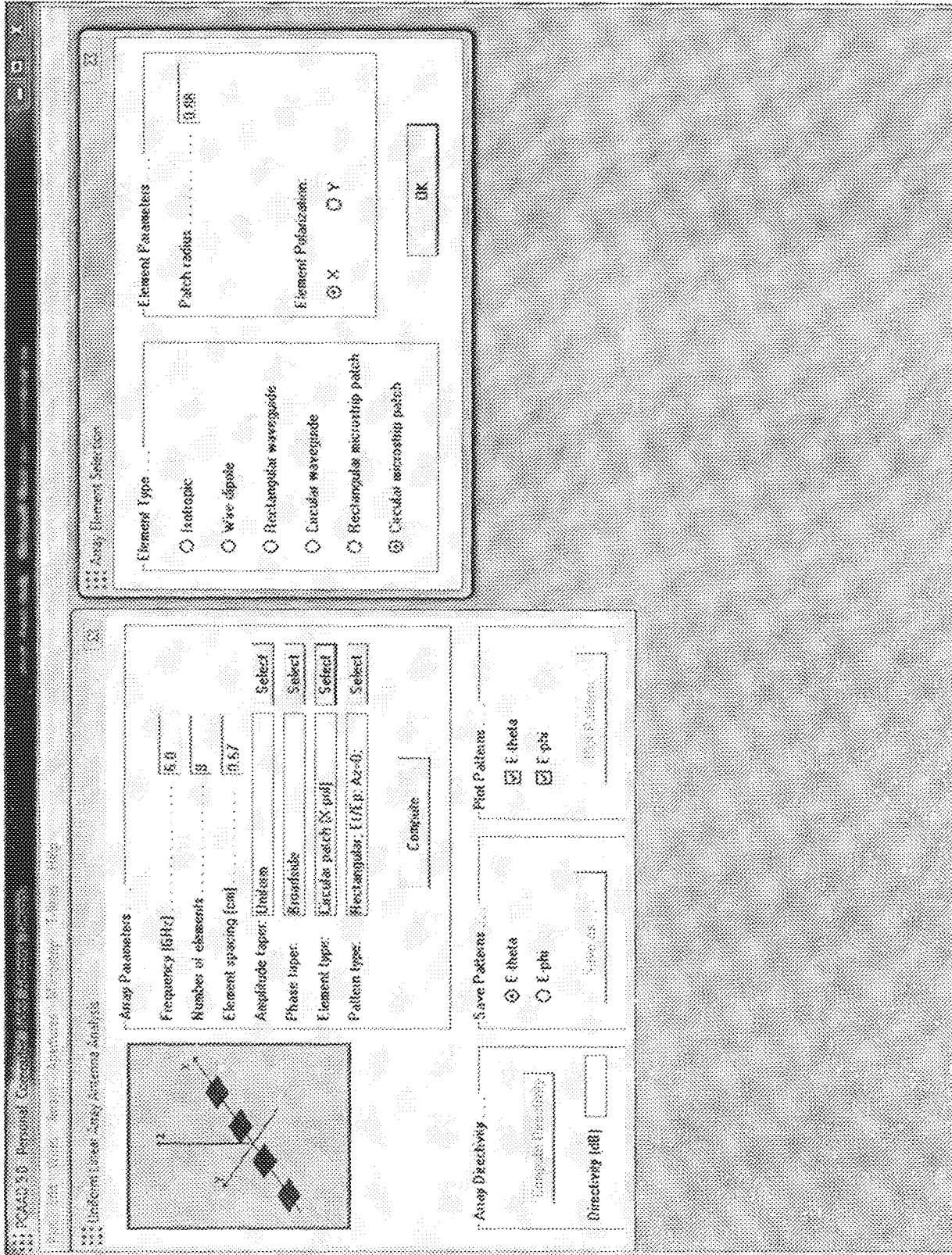
REFERENCES

- Alatan L. (2002), "*Design of Series Fed Circularly Polarized Microstrip Patch Array*", 2002 IEEE APS International Symposium and URSI Radio Science Meeting, Proc. APS, Vol.2, pp. 212-215
- Anitha V.R. and Reddy S. N. (2009), "*Design of an 8X1 Square Patch Antenna Array*", International Journal of Electronic Engineering Research Volume 1 Number 1 pp. 71-77
- Baars J. W. M. (2007), *The Paraboloidal Reflector Antenna in Radio Astronomy and communication, Theory and Practice*, Springer Science + Business Media, New York pp. 57-90
- Bahl Inder J. and Bhartia P. (2001), *Microstrip Antenna Design Handbook*, Artech House Inc. pp 720-731
- Balanis C.A. (2005), *Antenna Theory: Analysis and Design*, 3rd Edition John Wiley & Sons, Inc., Hoboken, New Jersey, pp. 70 - 944
- Cakir G. and Sevgi L. (2005), "*Design, Simulation and Tests of a Low-cost Microstrip Patch Antenna Arrays for the Wireless Communication*" Turkish Journal of Electrical Engineering, Vol.13, NO.1, pp 93-102
- Carr Joseph J. (2001), *Practical Antenna Handbook 4th Edition*, by the McGraw-Hill Companies, Inc. pp. 123-160
- Erel M. (2002), "*Design of microstrip patch antenna for the NPSATI*" Naval Postgraduate School Monterey, CA pp. 3-51
- Garg, R., Bhartia P., Bahl I. and Ittipiboon A. (2001), *Microstrip Antenna Design Handbook* Artech House Inc. Norwood MA, pp. 43-52,718-756
- Godara L. C., (2002) *Handbook of Antennas in Wireless Communications*, CRC Press LLC, New York, pp 195-215
- Keshitkar A., Dastkhosh A. R and Keshitkar A. (2008) "*Circular Microstrip Patch Array Antenna for C-Band Altimeter System*", International Journal of Antennas and Propagation, Volume 2008 pp. 1-7
- Keskilammi M. and Kivikoski M (2007), *Cylindrical Patch Antenna Array for RFID Applications*, Tampere University of Technology, Tampere, Finland pp.1-4
- Kraus J. D., (1988), *Antennas*, 2nd ed., McGraw-Hill New York, pp 19-25
- Kuchar A. (1996), "*Aperture Coupled Patch Antenna Array*" Institute for Telecommunications and Microwaves the University of Technology Vienna pp. 1-61

- Kumar, G. and Ray, K.P., (2003), *Broadband Microstrip Antennas*, Artech House Inc. Norwood MA pp.3-7
- Lai T.F, Mahadi W. N. L. and Soin N. (2008), "*Circular Patch Microstrip Array Antenna for KU-band*" World Academy of Science, Engineering and Technology 48 298 pp.2-6
- Merad L., Bendimerad F.T. and Meriah S.M., (2003), "*Genetic algorithm optimization for circular microstrip antenna*", ITG, INCA, Berlin pp. 1-3
- Michalewicz, Z. (1999), "*Genetic Algorithms + Data Structures = Evolution Programs*", Springer-Verlag, Berlin
- Michel C. (2004), "*Design of a UHF Circularly Polarized Patch Antenna as a feed for a 9.1 meter Parabolic Reflector*", Defense R&D Canada-Ottawa Technical Memorandum DRDC Ottawa TM 2004-139, pp. 1-19
- Milligan T. A., (2005), *Modern Antenna Design*, 2nd Ed, John Wiley & Sons, pp. 1-287
- Miron D. (2006), *Small Antenna Design*, Newnes, Burlington, MA pp. 603-640
- Orban D. and Moernaut G.J. (2005), "*The Basics of Patch Antennas*" www.orbanmicrowave.com
- Orfanidis S.J. (2008), *Electromagnetic Waves & Antennas*, Rutgers Univ. Press, New Brunswick, NJ, pp.603-630
- Pietrosemoli E. (2004), "*Geometry of Parabolic Reflectors*", Abdus Salam ICTP School on Digital Radio Communications for Research and Training in Developing Countries pp 1-16
- Pozar D.M. (1987), "*Increasing the Bandwidth of a Microstrip Antenna by Proximity Coupling*" *Electronics Letters*, Volume: 23, Issue: 8 pp. 368-369
- Reasoner H. (1989), "*Microwave Feeds for Parabolic Dishes*" *Proceedings of Microwave Update '89*, ARRL, pp. 75-84.
- Singer A. (2003), "*Feed design and selection for microwave antennas*", *Mobile Radio Technology 2003*, pp.1-3
- Wade P. (2003), "*Parabolic Dish Antennas*", *The WIGHZ Online Microwave Antenna*, Shirley, MA pp. 1-25

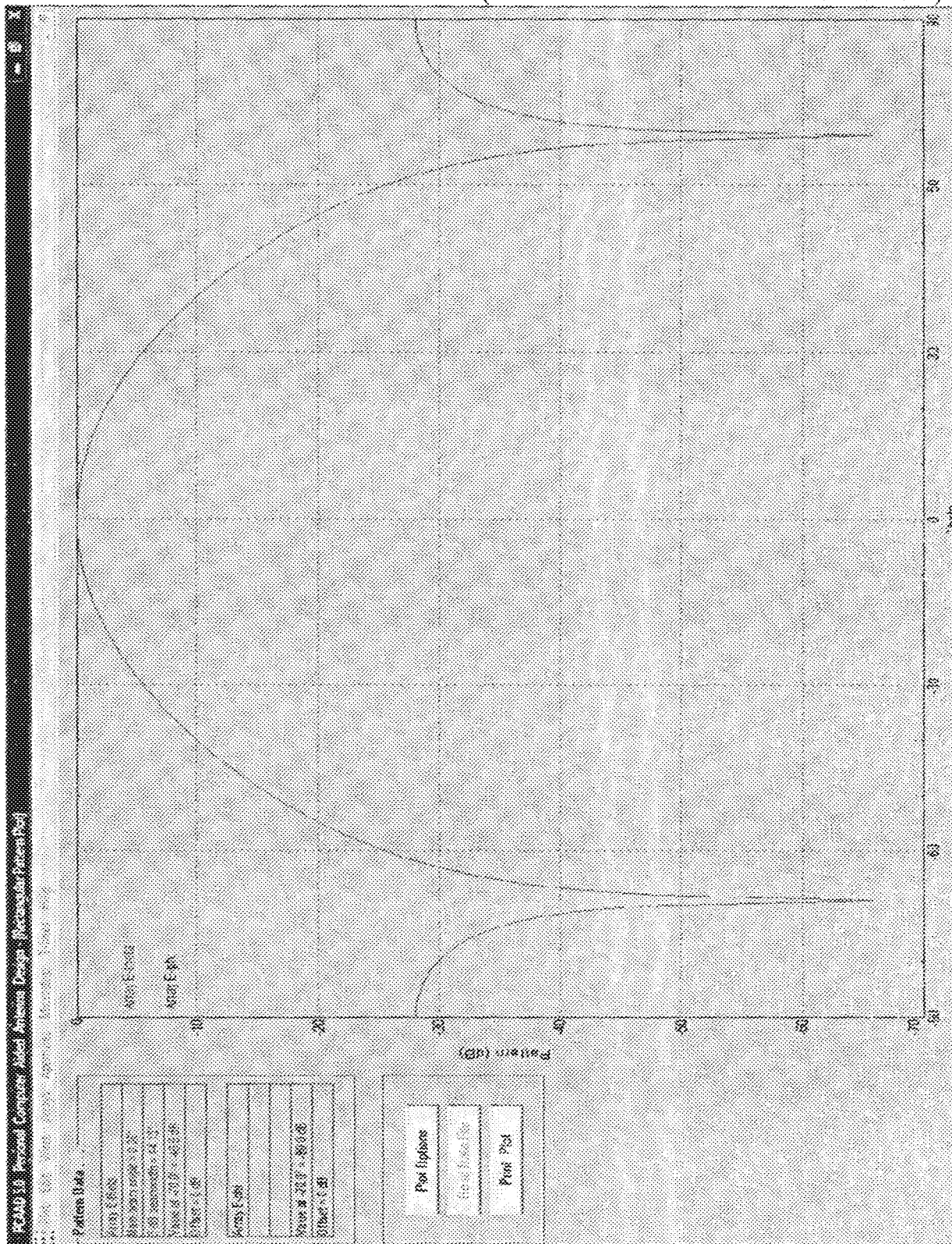
APPENDIX A

PCAAD 5.0 PC SCREEN DISPLAY (PARAMETER SPECIFICATION)



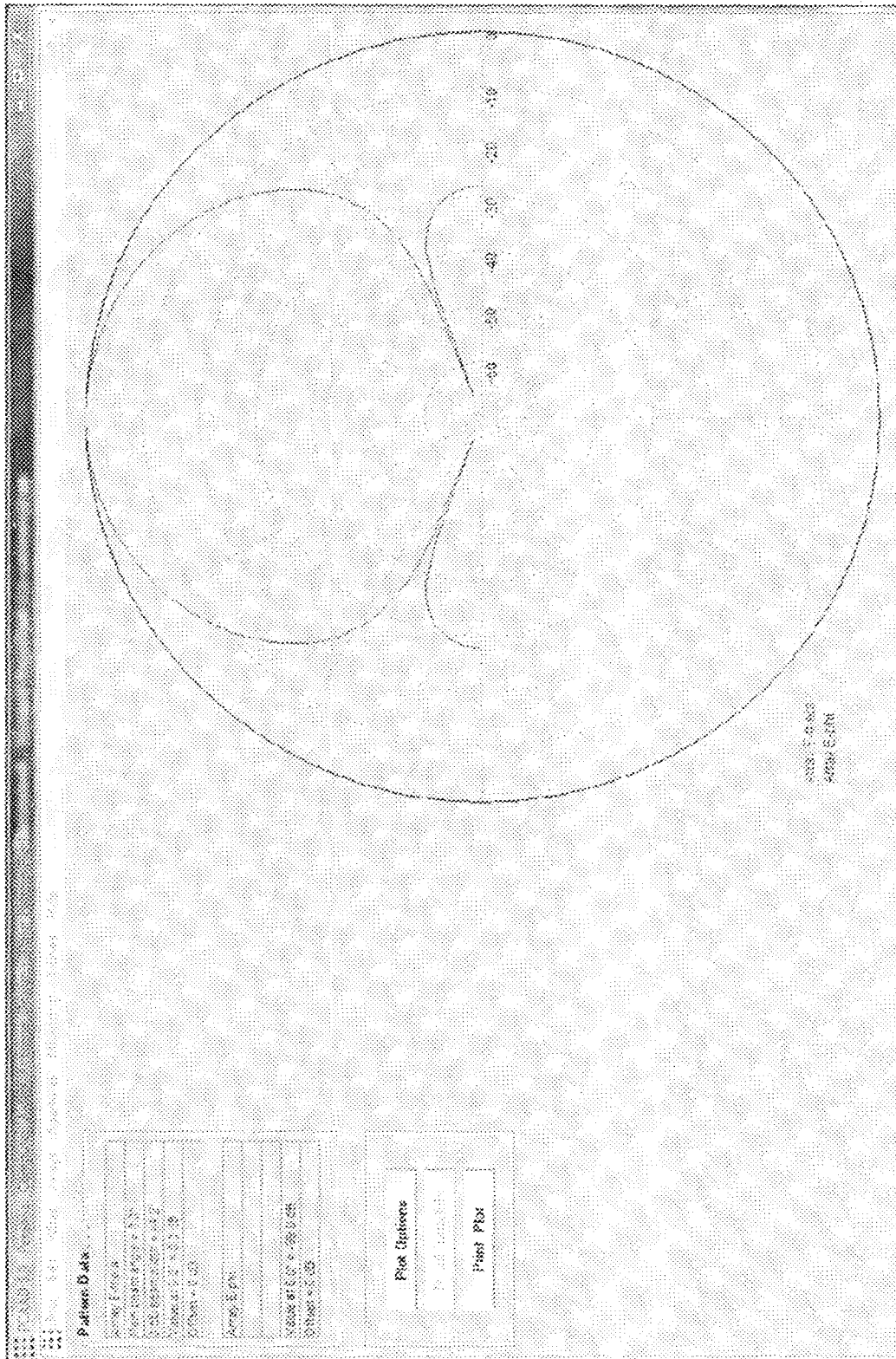
APPENDIX B

PCAAD 5.0 PC SCREEN DISPLAY (RECTANGULAR PLANAR PLOT)



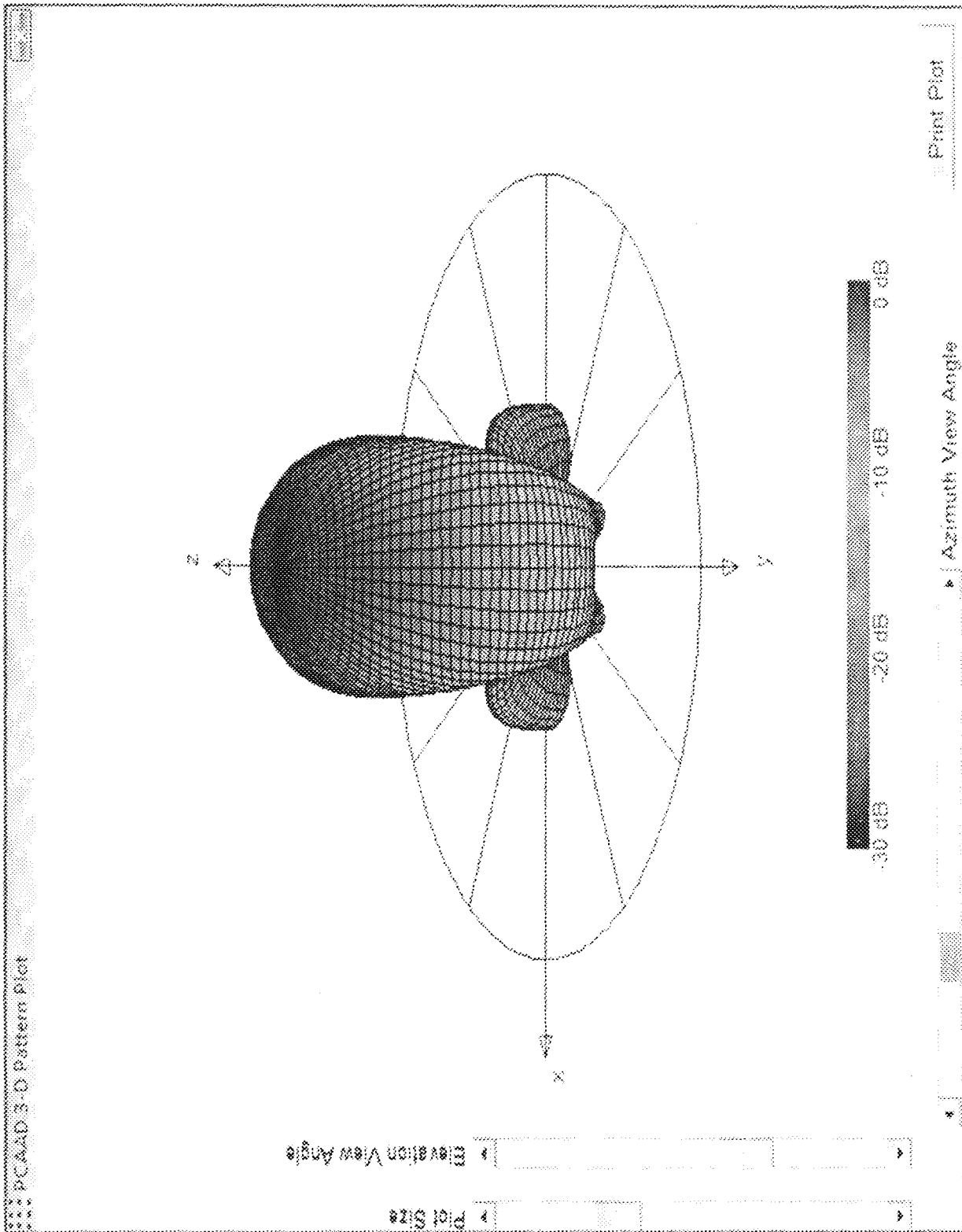
APPENDIX C

PCAAD 5.0 PC SCREEN DISPLAY (POLAR PLOT)



APPENDIX D

PCAAD 5.0 PC SCREEN DISPLAY (3-D PATTERN PLOT)



APPENDIX E

MATLAB SCRIPT FILE: FITNESS FUNCTION AND CONSTRAINT FOR THE OPTIMIZATION OF THE PATCH ANTENNA ARRAY FEED USING THE GENETIC ALGORITHM OPTIMIZATION TOOLBOX

```
% Matlab Code: Genetic algorithm optimization of the patch antenna array
feed. Fitness function and Constraint for optimization toolbox
% Date 02-July-2010
% Department of Electrical and Computer Engineering,
% Federal University of Technology, Minna
% Author : IBIGBAMI, OLUWOLE NELSON

function fitness = Sidelobe(chrom)
thet=0:0.01:20; % specifying the sidelobe before the first null
theta=deg2rad(thet);
d=0.67; % inter-element distance
% array factor expression
y=abs(chrom(1)*cos(0.5*1.26*d*cos(theta))+chrom(2)*cos(1.5*1.26*d*cos(theta))
+chrom(3)*cos(2.5*1.26*d*cos(theta))+chrom(4)*cos(3.5*1.26*d*cos(theta)));
sll1=trapz(theta,y); % integrating the sidelobes before first null
thet2=160:0.01:180;% specifying the sidelobe after first null
theta2=deg2rad(thet2);
% array factor expression
y2=abs(chrom(1)*cos(0.5*1.26*d*cos(theta2))+chrom(2)*cos(1.5*1.26*d*cos(theta2)
)+chrom(3)*cos(2.5*1.26*d*cos(theta2))+chrom(4)*cos(3.5*1.26*d*cos(theta2)));
sll2=trapz(theta2,y2); % integrating the sidelobes after first null
F1=sll1+sll2+max(y2)+max(y);%fitness function expression
thet3=20;% specifying first null constraint
theta3=deg2rad(thet3);
y3=abs(chrom(1)*cos(0.5*1.26*d*cos(theta3))+chrom(2)*cos(1.5*1.26*d*cos(theta3)
)+chrom(3)*cos(2.5*1.26*d*cos(theta3))+chrom(4)*cos(3.5*1.26*d*cos(theta3)));
thet4=160;% specifying first null constraint
theta4=deg2rad(thet4);
y4=abs(chrom(1)*cos(0.5*1.26*d*cos(theta4))+chrom(2)*cos(1.5*1.26*d*cos(theta4)
)+chrom(3)*cos(2.5*1.26*d*cos(theta4))+chrom(4)*cos(3.5*1.26*d*cos(theta4)));
F2=y3+y4;
fitness=F1+F2 %fitness function expression

function (c, ceq) = SLLconstraint(chrom)
d=0.67;
tet=20:0.01:160;
teta=deg2rad(tet);
tet2=0:0.01:180;
teta2=deg2rad(tet2);
y=chrom(1)*cos(0.5*1.26*d*cos(teta))+chrom(2)*cos(1.5*1.26*d*cos(teta))+chrom
(3)*cos(2.5*1.26*d*cos(teta))+chrom(4)*cos(3.5*1.26*d*cos(teta));
y2=chrom(1)*cos(0.5*1.26*d*cos(teta2))+chrom(2)*cos(1.5*1.26*d*cos(teta2))+ch
rom(3)*cos(2.5*1.26*d*cos(teta2))+chrom(4)*cos(3.5*1.26*d*cos(teta2));
z= trapz(teta,y);
z2= trapz(teta2,y2);
c=[];
ceq=z2-4.7433;
```

APPENDIX F

MATLAB SCRIPT FILE: APERTURE EFFICIENCY COMPUTATION

```
% Matlab Code: Aperture Efficiency versus Inter-element distance
% Radiated Power from feed versus Inter-element distance

% Date 02-July-2010
% Department of Electrical and Computer Engineering,
% Federal University of Technology, Minna

% Author : IBIGBAMI, OLUWOLE NELSON

clear all
close all
clc

% Initialising the aperture illumination angles
% recall that aperture illumination is 140 degrees
% which is from 20 to 160 degrees
thetAI1=20;
thetAI2=160;

% Computation of total power radiated from feed
totrad=quadv(@arafat,deg2rad(0),deg2rad(360));
totradpowr=10*log10(totrad);

% Computation of total radiation on effective aperture of dish
aparad=quadv(@arafat,deg2rad(thetAI1),deg2rad(thetAI2));
aparadpowr=10*log10(aparad);

% Plot of total radiation on effective aperture of dish and total
power radiated from feed against inter-element distance
plot(d,totradpowr),xlabel('inter-element distance(cm)'),
ylabel('total power radiated by feed(%)'),grid on
hold all
plot(d,aparadpowr),xlabel('inter-element distance(cm)'),
ylabel('power radiated on aperture(%)'),grid on
hold off
% plot of efficiency against inter-element distance
eff=100*(aparad./totrad);
plot(d,eff),xlabel('inter-element
distance(cm)'),ylabel('efficiency(%)'),grid on

% Call function arafact
function y = arafact(theta)
a1=1;a2=1;a3=1;a4=1;
d=0.4:0.025:1.4;
y=a1*cos(0.5*1.26*d*cos(theta))+a2*cos(1.5*1.26*d*cos(theta))+.....
a3*cos(2.5*1.26*d*cos(theta))+a4*cos(3.5*1.26*d*cos(theta));
```